



UNIVERSIDADE FEDERAL DE PERNAMBUCO  
CENTRO DE TECNOLOGIA E GEOCIÊNCIAS  
PROGRAMA DE PÓS-GRADUAÇÃO EM OCEANOGRAFIA – PPGO

JULIA GALETTI RODRIGUES

**CONTEÚDO DE OXIGÊNIO NO ATLÂNTICO TROPICAL SUDOESTE**

Recife  
2022

JULIA GALETTI RODRIGUES

## CONTEÚDO DE OXIGÊNIO NO ATLÂNTICO TROPICAL SUDOESTE

Dissertação apresentada ao Programa de Pós Graduação em Oceanografia da Universidade Federal de Pernambuco, como requisito parcial para a obtenção do título de Mestre em Oceanografia.

Área de concentração: Oceanografia.

**Orientador:** Prof. Dr. Moacyr Cunha de Araujo Filho

**Coorientador:** Prof. Dr. Arnaud Pierre Alexis Bertrand

Recife

2022

Catálogo na fonte  
Bibliotecário Gabriel Luz CRB-4 / 2222

R696c      Rodrigues, Julia Galetti.  
              Conteúdo de oxigênio no atlântico tropical sudoeste / Julia Galetti  
Rodrigues. 2022.  
              49 f: il.

              Orientador: Prof. Dr. Moacyr Cunha de Araujo Filho.  
              Coorientador: Prof. Dr. Arnaud Pierre Alexis Bertrand.  
              Dissertação (Mestrado) – Universidade Federal de Pernambuco. CTG.  
Programa de Pós-Graduação em Oceanografia, Recife, 2022.  
              Textos em inglês.  
              Inclui referências.

              1. Oceanografia. 2. Desoxigenação oceânica. 3. Atlântico Tropical  
Sudoeste. 4. Análise de dados funcionais. 5. Ventilação oceânica. 6.  
Subcorrente norte do Brasil. I. Araujo Filho, Moacyr Cunha de (Orientador). II.  
Bertrand, Arnaud Pierre Alexis (Coorientador). III. Título.

UFPE

551.46 CDD (22. ed.)

BCTG / 2022 - 439

JULIA GALETTI RODRIGUES

## **CONTEÚDO DE OXIGÊNIO NO ATLÂNTICO TROPICAL SUDOESTE**

Dissertação apresentada ao Programa de Pós Graduação em Oceanografia da Universidade Federal de Pernambuco, como requisito parcial para a obtenção do título de Mestre em Oceanografia.

Área de concentração: Oceanografia.

Aprovada em: 22/04/2022.

### **BANCA EXAMINADORA**

---

Prof. Dr. Moacyr Cunha de Araujo Filho (Orientador)  
Universidade Federal de Pernambuco

---

Prof. Dr. Alex Costa da Silva (Examinador Interno)  
Universidade Federal de Pernambuco

---

Dr<sup>a</sup>. Tonia Astrid Capuano (Examinador Externo)  
Institut de Recherche pour le Développement

---

Dr<sup>a</sup>. Ramilla Vieira de Assunção (Examinador Externo)  
Université de Bretagne Occidentale

## ABSTRACT

The Southwestern Tropical Atlantic (SWTA) is considered well oxygenated by the NBUC/NBC current system. Still, given the ongoing increase in ocean deoxygenation in the Eastern Tropical Atlantic (ETA), it is important to improve the knowledge on the current state of oxygen content in the SWTA. In this sense, we present the first three-dimensional representation of dissolved oxygen (DO) in the SWTA. Functional Data Analysis (FDA) was used to construct a database of DO profiles from two surveys (austral spring of 2015 and autumn of 2017) and complementary data from Pangea database. Results depicted three spatial areas with distinct oxygen content patterns, directly linked to the current systems: (i) Western Boundary Current System (WBCS) area, characterized by well oxygenated waters; (ii) South Equatorial Current System (SECS) area, containing the lowest DO values among all, and (iii) transition zone area, with intermediate DO content. We reveal that while the water column is fully oxygenated in the NBUC/NBC, WBCS oxygen content decreases at the limit of core as close as ~91 km (~50 km) from the coast in spring (autumn), due to the seasonal variability in NBUC/NBC intensity. Results also indicated that some processes are acting on the oxygen content in the study area, suggesting that the influence of the variability of the NBUC connection to the SEUC flow may feed subsurface westward transport of DO rich waters. Furthermore, a seasonal latitudinal displacement of the SEUC core could influence the distribution of the observed low oxygen waters, as well as allow the NBUC retroflexion to occur. Lastly, these findings highlight the importance of the western boundary current in maintaining the oxygenation and keeping the westward advected deoxygenated waters from reaching the shore.

**Keywords:** ocean deoxygenation; southwestern Tropical Atlantic; functional data analysis; ventilation; North Brazilian Undercurrent.

## RESUMO

O Atlântico Tropical Sudoeste (ATSO) é considerado bem oxigenado pelo sistema das correntes Subcorrente/Corrente Norte do Brasil (SCNB/CNB). Ainda assim, dado o aumento contínuo da desoxigenação oceânica no Atlântico Tropical Leste, é importante aprimorar o conhecimento sobre o atual estado do conteúdo de oxigênio no ATSO. Neste sentido, apresentamos a primeira representação tridimensional do oxigênio dissolvido (OD) no ATSO. A Análise de Dados Funcionais (ADF) foi utilizada para construir um banco de dados de perfis de OD a partir de duas campanhas oceanográficas (Primavera de 2015 e Outono de 2017 austrais) e dados complementares da base de dados Pangea. Os resultados retrataram três áreas espaciais com padrões distintos de conteúdo de oxigênio, diretamente ligados aos sistemas de correntes: (i) área do Sistema de Correntes da Borda Oeste (SCBO), caracterizada por águas bem oxigenadas; (ii) área da Sistema de Correntes Sul Equatoriais (SCSE), contendo os menores valores de OD entre todos, e (iii) área da zona de transição, com conteúdo intermediário de OD. Revelamos que enquanto a coluna de água é totalmente oxigenada na SCNB/CNB, o conteúdo de oxigênio do SCBO diminui no limite do núcleo tão próximo a ~91 km (~50 km) da costa na primavera (outono), devido à variabilidade sazonal na intensidade da SCNB/CNB. Os resultados também indicaram que alguns processos estão atuando sobre o conteúdo de oxigênio na área de estudo, sugerindo que a influência da variabilidade da conexão da SCNB ao fluxo da Subcorrente Sul Equatorial (SSE) pode alimentar o transporte subsuperficial para oeste de águas ricas em OD. Além disso, um deslocamento latitudinal sazonal do núcleo da SSE poderia influenciar a distribuição das águas com baixo teor de oxigênio observadas, bem como permitir a retroflexão da SCNB. Finalmente, estas descobertas destacam a importância dos limites do SCBO para a manutenção da oxigenação e impedir que as águas desoxigenadas advindas do oeste cheguem à costa.

**Palavras-chave:** desoxigenação oceânica; Atlântico Tropical Sudoeste; análise de dados funcionais; ventilação oceânica; Subcorrente Norte do Brasil.

## LISTA DE ILUSTRAÇÕES

### DISSERTAÇÃO

- Figure 1 – Low and declining oxygen levels ( $<2\text{mg.l}^{-1}$ , red dots) in the open ocean and coastal waters, as well as ocean OMZs at 300 m of depth (blue shaded regions). 11
- Figure 2 – Representation of the mean currents in the Northeast Brazilian coast. Surface currents in red and subsurface currents in blue. The black rectangle indicates the NBUC-NBC transition zone. 14

### MANUSCRIPT I – OXYGEN CONTENT IN THE SOUTHWESTERN TROPICAL ATLANTIC

- Figure 1 – Study area in the southwestern tropical Atlantic (SWTA). Circles: ABRAÇOS data; Lozenges: PANGAEA datasets. Green full symbols: spring data; Red empty symbols: autumn data. The continental shelf is represented in white; the dashed line represents the shelf break (60 m isobath). RA: Rocas Atoll; FN: Fernando de Noronha archipelago. 20
- Figure 2 – Flowchart describing the Functional Data Analyses approach and the 3D representation of the oxygen content. 22
- Figure 3 – Score of the first two fPCA components (a, e) and clustering (b, f) analyses achieved on DO profiles. Spatial distribution of the clusters (c, g) and mean DO profile for each area (d, h) with the variation over the mean profiles represented by the dashed and continuous lines. Spring: a-d; Autumn: e-h. 25
- Figure 4 – Score of the first two fPCA components (a, e) and clustering (b, f) analyses achieved on DO profiles. Spatial distribution of the clusters (c, g) and mean DO profile for each area (d, h) with the variation over the mean profiles represented by the dashed and continuous lines. Spring: a-d; Autumn: e-h. 26
- Figure 5 – Validation of Functional Ordinary Kriging of the DO profiles for spring (a, b, c) and autumn (d, e, f) using Mean Square Difference (MSD). Distribution of MSD for all DO profiles (a,

	d). Examples of good (emphasised blue dots, a, d; continuous green line, b, e) and poor (emphasised red dots, a, d; dashed green lines, b, e) predictions of observed DO profiles (orange lines) for spring (a, b) and autumn (d, e). Boxplots of the MSD between observed and predicted over/under all model predictions for both seasons (c, f).	28
Figure 6 –	Dissolved oxygen in spring (a, c, e) and autumn (b, d, f) at 10 m (a, b), 190 m (c), 110 m (d) and 330 m (e, f) in the SWTA. The continental shelf is limited by the 60 m isobath represented in light grey. RA: Rocas Atoll; FN: Fernando de Noronha archipelago. The oxygen scale varies from 1.5 ml.l <sup>-1</sup> to 5 ml.l <sup>-1</sup> .	29
Figure 7 –	3D interpolation of DO using ordinary functional kriging. In spring (upper) interpolation relied on transects along-shelf (3.05°S/34.75°W – 7.25°S/34.25°W and 7.25°S/34.25°W – 9.05°S/34.30°W), along-shore (3.05°S/34.65°W – 5.55°S/34.55°W), and cross-shore over the islands (4.05°S/34.60°W – 3.95°S/32.15°W) and over the transition zone (4;95°S/31.45°W – 5.05°S/29.95°W). In autumn (lower) interpolation relied on transects along-shelf (4.95°S/34.95°W – 7.65°S/34.30°W and 7.65°S/34°W – 9.25°S/34.75°W), along-shore (3.45°S/34.45°W – 5.55°S/34.55°W), and cross-shore over the islands (4.15°S/36.25°W – 3.65°S/31.75°W) and over the transition zone (5.65°S/34.85°W – 5.05°S/31.55°W)	31
Figure S1 –	Functional ANOVA (spring: b, d; autumn: f, h) between the DO profiles from different databases (spring: a, c; autumn: e, g) within each area classified from the reference dataset.	42
Figure S2 –	Variogram for Functional Ordinary Kriging in spring (left) and autumn (right).	43



## LISTA DE TABELAS

### MANUSCRIPT I – OXYGEN CONTENT IN THE SOUTHWESTERN TROPICAL ATLANTIC

Table 1 –	Number of profiles selected from each database in austral spring and autumn.	21
-----------	---	----

## LISTA DE ABREVIATURAS E SIGLAS

AAIW	Antarctic Intermediate Water
cSEC	Central branch of South Equatorial Current
Nsec	northern branch of the South Equatorial Current (nSEC)
DO	Dissolved oxygen
ETA	Eastern Tropical Atlantic
ETNA	Eastern Tropical North Atlantic
ETSA	Eastern Tropical South Atlantic
EUC	Equatorial Undercurrent
FDA	Functional Data Analysis
NBC	North Brazil Current
NBUC	North Brazil Undercurrent
NECC	North Equatorial Counter Current
NEUC	North Equatorial Counter Undercurrent
OMZs	Oxygen Minimum Zones
SACW	South Atlantic Central Water
SECS	South Equatorial Current System
SEUC	South Equatorial Undercurrent
SWTA	Southwest Tropical Atlantic
WBCS	Western Boundary Current System

## **SUMÁRIO**

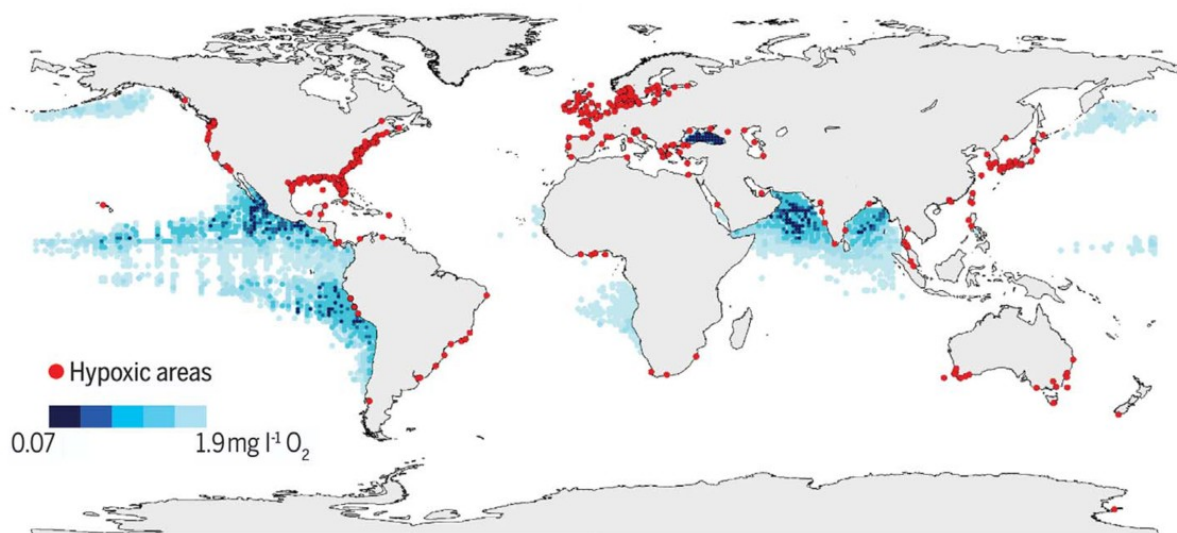
<b>1</b>	<b>INTRODUCTION</b>	<b>11</b>
<b>2</b>	<b>OBJECTIVES</b>	<b>16</b>
2.1	GENERAL	16
2.2	SPECIFICS	16
<b>3</b>	<b>MANUSCRIPT I – OXYGEN CONTENT IN THE SOUTHWESTERN TROPICAL ATLANTIC</b>	<b>17</b>
<b>4</b>	<b>FINAL CONSIDERATIONS</b>	<b>44</b>
	<b>REFERENCES</b>	<b>45</b>

## 1 INTRODUCTION

Dissolved oxygen (DO) structures the ocean by influencing productivity, biodiversity, biogeochemical cycles, ocean/atmosphere interactions and further impact on climate regulation (BREITBURG et al., 2018; KEELING et al., 2010; STRAMMA et al., 2008). The effects of DO over this structure is a consequence of the delicate balance between production/consumption and ventilation processes, which can be driven at different scales by both physical and biogeochemical mechanisms (DUTEIL et al., 2018; LÖSCHER et al., 2016; OSCHILES et al., 2018; REN et al., 2018; STRAMMA et al., 2009).

Ocean oxygen content has decreased substantially in recent decades (BREITBURG et al., 2018; KEELING et al., 2010; SCHMIDTKO et al., 2017; SHEPHERD et al., 2017) and an increase in deoxygenation is forecasted in a warmer ocean (KEELING et al., 2010; SCHMIDTKO et al., 2017; STRAMMA et al., 2008). The increase in surface temperature decreases the solubility of oxygen in the ocean. A more stratified water column has reduced ventilation (OSCHILES et al., 2018), decreasing the input of dissolved oxygen (DO) from the surface to deeper layers of the oceans (BREITBURG et al., 2018; REN et al., 2018; SHEPHERD et al., 2017).

Figure 1 – Low and declining oxygen levels ( $<2\text{mg.l}^{-1}$ , red dots) in the open ocean and coastal waters, as well as ocean OMZs at 300 m of depth (blue shaded regions).



Source: Breitburg (2018, p. 1).

In regions where deoxygenation rates are persistent, Oxygen Minimum Zones (OMZs) lie within shaded areas of the ventilated thermocline (LUYTEN et al., 1983), separated from the well-oxygenated mixed layer by strong vertical DO gradients (KARSTENSEN et al., 2008). These zones are distributed more specifically in the tropical zones of the Pacific and Atlantic oceans (BRANDT et al., 2015; KARSTENSEN et al., 2008; LÖSCHER et al., 2016; STRAMMA et al., 2008, 2009), in the North Atlantic (RHEIN et al., 2017), in the North Pacific (PRAETORIUS et al., 2015) and the North Indian Ocean (NAQVI et al., 2006).

There is no DO concentration threshold that defines an OMZ. Since they vary spatially with physical and biogeochemical drivers, these zones are defined when an abrupt change in DO content and very low oxygen concentrations occur. The North Atlantic OMZ oxygen content is set by concentrations of less than  $40 \mu\text{mol.kg}^{-1}$ , while in the South Atlantic is less than  $17 \mu\text{mol.kg}^{-1}$  (KARSTENSEN et al., 2008). In this sense, generally three terms are used to describe general oxygen conditions: anoxic, suboxic, and oxic. Anoxic conditions refer to the absence of DO, while suboxide to low DO concentrations, although triggering different biogeochemical processes (KARSTENSEN et al., 2008). In the Atlantic the smaller volume and higher ventilation in comparison to the Pacific entails more flexible values to define the OMZs DO threshold (KARSTENSEN et al., 2008).

Regardless of the classification, the sensitivity of marine organisms, especially macroorganisms, to the content of dissolved oxygen is highly non-linear, varying between different species and oxygen concentrations (KEELING et al., 2010). Under hypoxic conditions (below  $\sim 60 - 120 \mu\text{mol.kg}^{-1}$ ) macroorganisms become stressed or even die (STRAMMA et al., 2008). Organisms need both food and oxygen, and in some circumstances, the second may be more difficult to obtain than the first (PAULY AND KINNE, 2010). The increased stratification of the water column also implies a reduction in the vertical extent of the mixing layer, and thus a shallower thermocline (OSCHLIES et al., 2018). This implies reduced habitat for marine species that depend on well-oxygenated waters (BERTRAND et al., 2010). As oxygen depletion becomes more intense and persistent, the oceans lose their ability to support high biomass and ecosystem functioning is compromised, affecting the trophic web (BREITBURG et al., 2018). Furthermore the rates of growth, survival, reproduction, visual ability and immune responses of marine organisms could decrease, because they are forced to use most of their energy for vital functions

(SEIBEL, 2011). Although there are many biogeochemical processes that remove oxygen from the water column, here we are interested in the connection between oxygen distribution and physical processes.

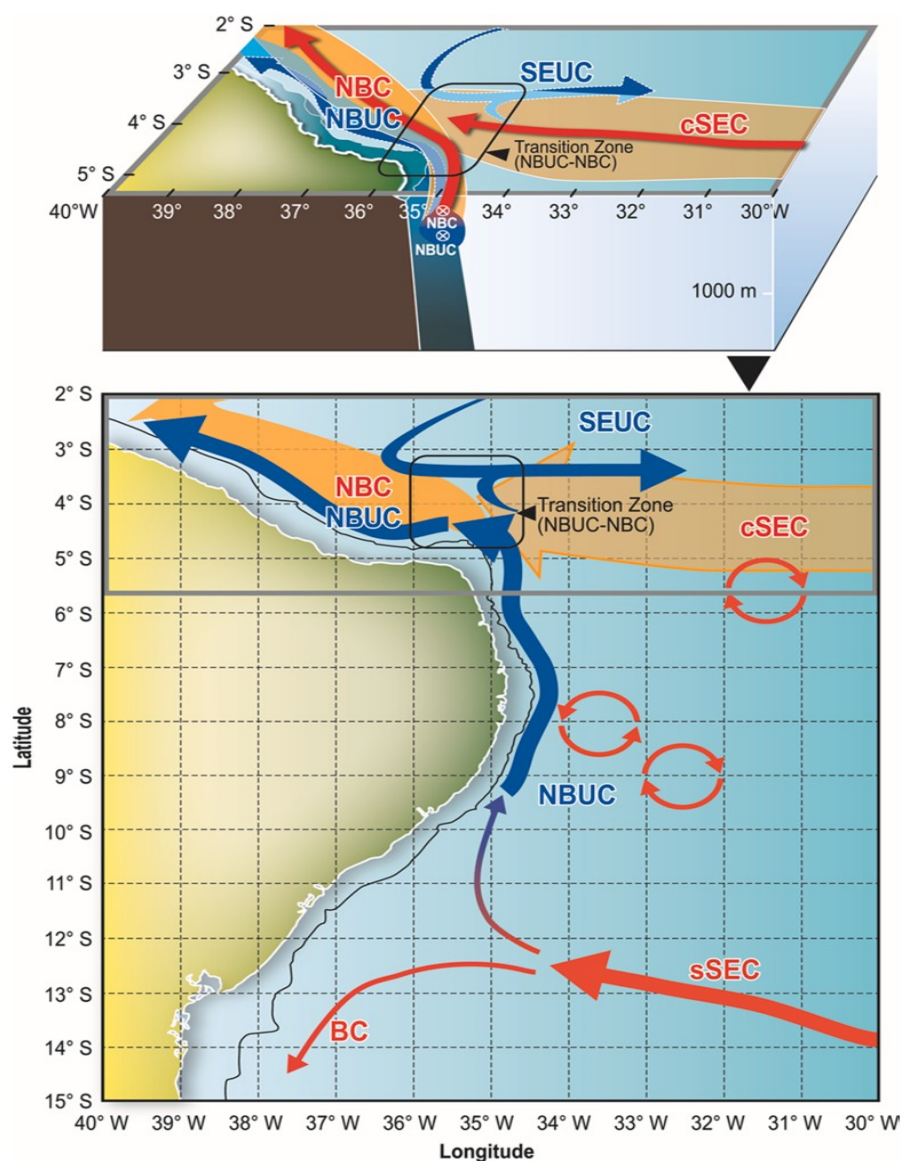
Research on deoxygenation in the tropical oceans have been conducted mostly on the Eastern Boundary Upwelling Systems (EBUS), where the most intense OMZs occur (BREITBURG et al., 2018; DUTEIL et al., 2018; GALLO et al., 2016; KEELING et al., 2010; LEVIN, 2017; OSCHILES et al., 2018; SCHMIDTKO et al., 2017; SHEPHERD et al., 2017). Favored by respiration rates higher than the photosynthetic production and low DO supply due to slow ventilation, OMZs play an important role in the global biogeochemical cycle and present specific ecosystem structure and fisheries (BERTRAND et al., 2011; PRINCE et al., 2010; VAQUER-SUNYER et al., 2008).

In the Tropical Atlantic, the lowest DO concentrations are found in the Eastern Tropical North and South Atlantic (ETNA and ETSA) (BRANDT et al., 2010, 2015; HAHN et al., 2017; KARSTENSEN et al., 2008; LÖSCHER et al., 2015; STRAMMA et al., 2009). Even though deoxygenated waters are transported towards the Western Boundary Current System (WBCS) by surface and thermocline current branches (BRANDT et al., 2010), the oxygen content increases towards the western boundary. The western Atlantic Ocean is characterised by relatively high oxygen content plays a role in oxygenating the Eastern Tropical Atlantic (ETA) (BRANDT et al., 2015). Oxygen-rich waters are supplied toward the eastern Atlantic between the surface mixed layer and  $\sigma\theta = 27.1 \text{ kg m}^{-3}$ , which corresponds to the South Atlantic Central Water (SACW) and the Antarctic Intermediate Water (AAIW) interface (BRANDT et al., 2008; STRAMMA et al., 2009). The main currents associated to those limits are: (i) the Equatorial Undercurrent (EUC,  $\sim 0 - 200 \text{ m}$ ), dominating the zonal flow of the Equatorial Atlantic; (ii) the weaker eastward North Equatorial Counter Current/Undercurrent (NECC/NEUC); and (iii) the South Equatorial Undercurrent (SEUC;  $\sim 4.5^\circ\text{S}$ ;  $\sim 100 - 400 \text{ m}$ ) (BRANDT et al., 2010).

The circulation along the northeast Brazilian coast is dominated by the Western Boundary Current System (WBCS) comprised by the North Brazil Undercurrent (NBUC) and the North Brazil Current (NBC) (DA SILVEIRA AND BROWN, 2000; DOSSA et al., 2021). At  $\sim 5^\circ\text{S}$  the NBUC is intensified by the central branch of South Equatorial Current (cSEC) giving origin to the surface-intensified NBC west of  $35^\circ\text{W}$  (DOSSA et al., 2021; DA SILVEIRA, 1994; STRAMMA et al.,

1995). The NBUC continues subsurface flowing equatorward together with the NBC (DOSSA et al., 2021), both carrying oxygenated central and intermediate water masses (SACW and AAIW) (BRANDT et al., 2015). Part of the NBC waters will further retroflect and feed the North Equatorial Countercurrent (NECC,  $\sim 9^\circ\text{N}$ ) and Undercurrent (NEUC,  $\sim 5^\circ\text{N}$ ), which will then feed the northern branch of the South Equatorial Current (nSEC) (DA SILVEIRA AND BROWN, 2000).

Figure 2 – Representation of the mean currents in the Northeast Brazilian coast. Surface currents in red and subsurface currents in blue. The black rectangle indicates the NBUC-NBC transition zone.



Source: Dossa (2020, p. 2).

Although much is known about the mechanisms involved in oxygenation/deoxygenation in the ETA, little is known about the WBCS. Considering the current trends in deoxygenation and global expansion of OMZs (SCHMIDTKO et

al., 2017; STRAMMA et al., 2008;), it is necessary to have a baseline on DO conditions in the Southwestern Tropical Atlantic (SWTA). In this context, we propose the first three-dimensional representation of DO in the SWTA. For that purpose we took advantage of two surveys conducted in SWTA in austral spring 2015 (BERTRAND, 2015) and autumn 2017 (BERTRAND, 2017) in combination with another available database (PANGAEA, <https://www.pangaea.de/>).



## 2 OBJECTIVES

### 2.1 GENERAL

Characterize the three-dimensional structure of the oxygen content in Southwestern Tropical Atlantic for spring and autumn.

### 2.2 SPECIFICS

- (I) Optimize the available information on dissolved oxygen in the Tropical Atlantic for spring and autumn, using the Functional Data Analysis technique;
- (II) Investigate whether the seasonality of the Northern Brazil Undercurrent influences the distribution of oxygen concentration in the SWTA and how;
- (III) Identify which oceanic processes are acting on the DO content variability.

### 3 MANUSCRIPT I: Oxygen content in the Southwestern Tropical Atlantic

Manuscript submitted to the Regional Studies in Marine Science Journal

#### Abstract

The Southwest Tropical Atlantic (SWTA) is considered well oxygenated by the North Brazil Undercurrent/North Brazil Current (NBUC/NBC) system. Still, given the ongoing increase in ocean deoxygenation in the Eastern Tropical Atlantic (ETA), it is important to improve the knowledge on the current state of oxygen content in the SWTA. In this sense, we present the first three-dimensional representation of dissolved oxygen (DO) in the SWTA. Functional Data Analysis (FDA) was used to construct a database of DO profiles from two surveys (austral spring of 2015 and autumn of 2017) and a complementary database. Results depicted three spatial areas with distinct oxygen content patterns, directly linked to the current systems: (i) Western Boundary Current System (WBCS) area, characterized by well oxygenated waters; (ii) South Equatorial Current System (SECS) area, containing the lowest DO values among all, and (iii) transition zone area, with intermediate DO content. We reveal that while the water column is fully oxygenated in the region of the core of the NBUC/NBC, WBCS oxygen content decreases at the limit of the core as close as ~91 km (~50 km) from the coast in spring (autumn), related to the seasonal variability in NBUC/NBC intensity. Results also indicated that other processes are acting on the oxygen content in the study area, suggesting that the influence of the variability of the NBUC connection to the SEUC flow may feed subsurface westward transport of DO rich waters. Finally, these findings highlight the importance of the western boundary current in maintaining the oxygenation and keeping the westward advected deoxygenated waters from reaching the shore.

**Keywords:** ocean deoxygenation; southwestern Tropical Atlantic; functional data analysis; ventilation; North Brazilian Undercurrent system.

#### 1. Introduction

Dissolved oxygen (DO) plays a structuring role in the ocean given its influence on productivity, biodiversity, biogeochemical cycles, ocean/atmosphere interactions and further impact on climate regulation (Breitburg et al., 2018; Keeling et al., 2010; Stramma et al., 2008). Ocean oxygen content is a consequence of the delicate balance between production/consumption and ventilation processes. These effects

can be driven by both physical and biogeochemical mechanisms at different scales (Duteil et al., 2018; Löscher et al., 2016; Oschiles et al., 2018; Ren et al., 2018; Stramma et al., 2009). Ocean oxygen content has decreased substantially in recent decades (Breitburg et al., 2018; Keeling et al., 2010; Schmidtko et al., 2017; Shepherd et al., 2017) and an increase in deoxygenation is forecasted in a warmer ocean (Keeling et al., 2010; Schmidtko et al., 2017; Stramma et al., 2008). Indeed, oxygen solubility in seawater decreases with the temperature while increased stratification hampers ventilation (Oschiles et al., 2018). In regions where deoxygenation rates are persistent, Oxygen Minimum Zones (OMZs) lie within shaded areas of the ventilated thermocline (Luyten et al., 1983), separated from the well-oxygenated mixed layer by strong vertical DO gradients (Karstensen et al., 2008).

In tropical oceans, research on deoxygenation have been mostly focusing on the major Eastern Boundary Upwelling Systems (EBUS), where the most intense OMZs occur (Breitburg et al., 2018; Duteil et al., 2018; Gallo et al., 2016; Keeling et al., 2010; Levin, 2017; Oschiles et al., 2018; Schmidtko et al., 2017; Shepherd et al., 2017). Favored by respiration rates higher than the photosynthetic production and low DO supply due to slow ventilation, OMZs play important role in global biogeochemical cycle and present specific ecosystem structure and fisheries (Bertrand et al., 2011; Prince et al., 2010; Vaquer-Sunyer et al., 2008). Although OMZs are bounded by steep oxygen gradients, deoxygenated waters are not restricted to OMZs.

In the Tropical Atlantic, the lowest DO concentrations are found in the Eastern Tropical North and South Atlantic (ETNA and ETSA), with oxygen content increasing westward (Brandt et al., 2010, 2015; Hahn et al., 2017; Karstensen et al., 2008; Löscher et al., 2015; Stramma et al., 2009). Deoxygenated waters are transported towards the Western Boundary Current System (WBCS) by surface and thermocline current branches (Brandt et al., 2010). Still, the western Atlantic Ocean is characterised by relatively high oxygen content at all latitudes and plays a role in oxygenating the Eastern Tropical Atlantic (ETA) (Brandt et al., 2015). The main pathways along which oxygen-rich waters are supplied toward the eastern Atlantic are bounded between the surface mixed layer and  $\approx 27.1 \text{ kg m}^{-3}$ , which corresponds to the South Atlantic Central Water (SACW) and the Antarctic Intermediate Water

(AAIW) interface (Brandt et al., 2008; Stramma et al., 2009). The main currents associated to those limits are: (i) the Equatorial Undercurrent (EUC,  $\sim 0 - 200$  m), dominating the zonal flow of the Equatorial Atlantic; (ii) the weaker eastward North Equatorial Counter Current/Undercurrent (NECC/NEUC); and (iii) the South Equatorial Undercurrent (SEUC;  $\sim 4.5^\circ\text{S}$ ;  $\sim 100 - 400$  m) (Brandt et al., 2010).

The circulation along the northeast Brazilian coast is dominated by the Western Boundary Current System (WBCS) comprised by the North Brazil Undercurrent (NBUC) and the North Brazil Current (NBC) (da Silveira and Brown, 2000; Dossa et al., 2021). At  $\sim 5^\circ\text{S}$  the NBUC is intensified by the central branch of South Equatorial Current (cSEC) giving origin to the surface-intensified NBC west of  $35^\circ\text{W}$  (Dossa et al., 2021; da Silveira, 1994; Stramma et al., 1995). The NBUC continues in subsurface flowing equatorward together with the NBC (Dossa et al., 2021), both carrying oxygenated central and intermediate water masses (SACW and AAIW) (Brandt et al., 2015).

Although much is known about the mechanisms involved in oxygenation/deoxygenation in the ETA, little is known about the WBCS. Considering the current trends in deoxygenation and global expansion of OMZs (Schmidt et al., 2017; Stramma et al., 2008;), it is necessary to have a baseline on DO conditions in the Southwestern Tropical Atlantic (SWTA). In this context, we propose the first three-dimensional representation of DO in the SWTA. For that purpose, we took advantage of two surveys conducted in SWTA in austral spring 2015 (Bertrand, 2015) and autumn 2017 (Bertrand, 2017) in combination with another available database (PANGAEA).

## **2. Materials and Methods**

### **2.1. Data**

The reference dataset (Table 1) was acquired using a Conductivity, Temperature, Depth (CTD) Sea-bird SBE911 equipped with dissolved oxygen auxiliary sensor (SBE43) during two multidisciplinary cruises (Fig. 1) carried out on board the R/V Antea in the SWTA (between  $3^\circ\text{S}$ - $10^\circ\text{S}$  and  $30^\circ\text{W}$ - $36^\circ\text{W}$ ) as part of the Acoustic along the Brazilian Coast (ABRAÇOS) project. The first cruise (ABRAÇOS 1, Bertrand, 2015) was performed in September – October 2015 (austral spring) and the second (ABRAÇOS 2, Bertrand, 2017) in April – May 2017 (austral autumn).

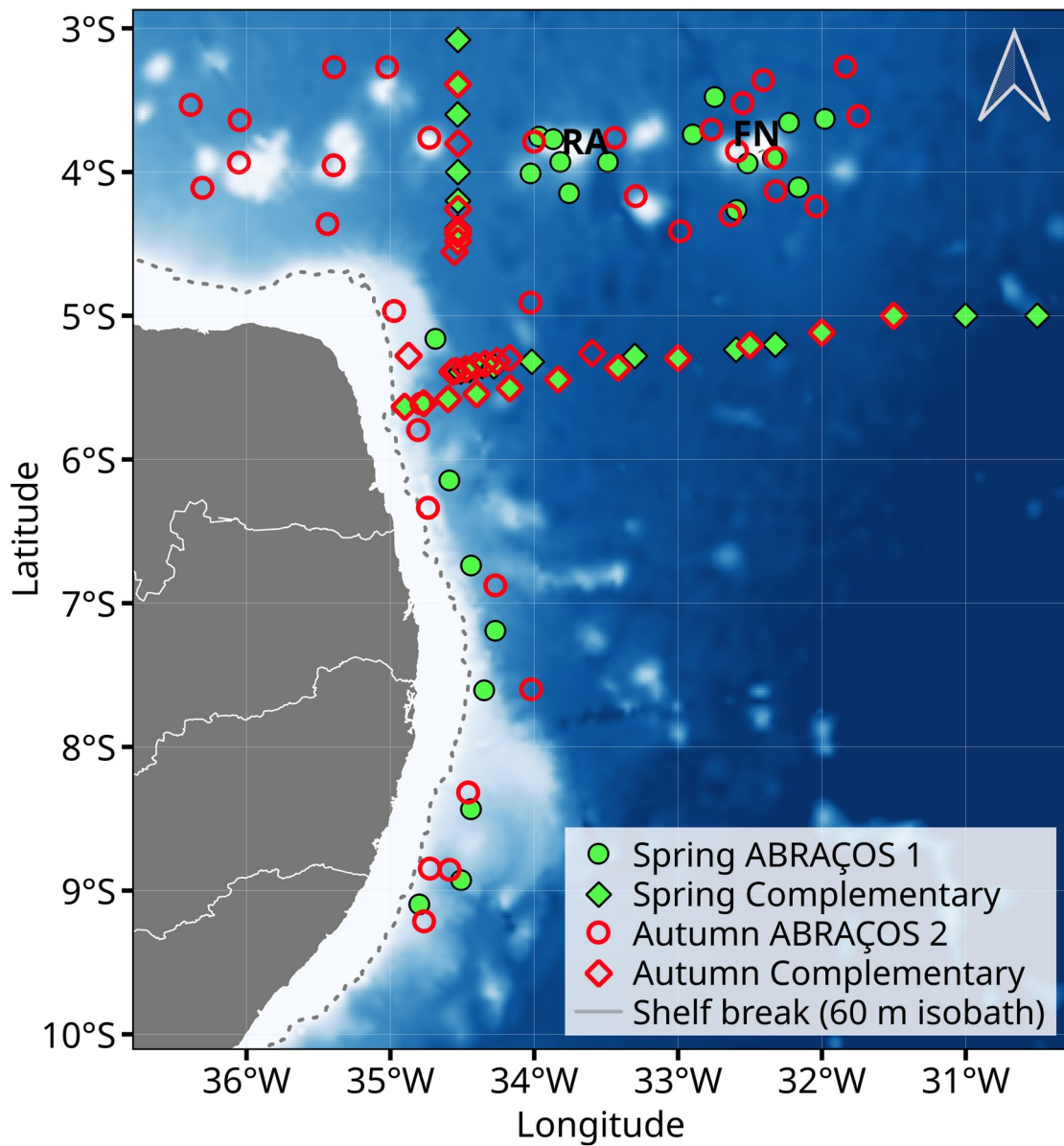


Figure 1 – Study area in the southwestern tropical Atlantic (SWTA). Circles: ABRAÇOS data; Lozenges: PANGAEA datasets. Green full symbols: spring data; Red empty symbols: autumn data. The continental shelf is represented in white; the dashed line represents the shelf break (60 m isobath). RA: Rocas Atoll; FN: Fernando de Noronha archipelago.

To improve the spatial coverage, following the methodology developed by Assunção et al. (2020), we also considered 56 complementary DO profiles extracted from PANGAEA (<https://www.pangaea.de/>), an open access library aimed at archiving, publishing and distributing georeferenced data from earth system research (Table 1; Fig. 1). Complementary data were selected for the same months of the ABRAÇOS

surveys but in other years. Only DO profiles at least 900 m and 600 m deep were considered for spring and autumn, respectively. All DO profiles were converted to  $\text{mL.l}^{-1}$ .

Tabela 1 – Number of profiles selected from each database in austral spring and autumn.

Database	Number of profiles (year of acquisition)	
	Spring	Autumn
ABRAÇOS	22 (2015)	34 (2017)
PANGEA	29 (1990, 2016)	27 (2000, 2014)

## 2.2. Functional Data Analysis

DO profiles were analysed using a Functional Data Analysis (FDA) approach (Ramsay and Silverman, 2005). FDA is a branch of statistics that allows highlighting the main features, patterns, and sources of variation of curves or surfaces (Ruiz-Medina, 2012). Since FDA allows describing and modelling sets of parameterized functions (or curves) rather than a sequence of individual observations (scalars or vectors), the methodology allows capturing linear dependencies between functions, revealing standardized behaviours between different curves (Giraldo et al., 2011). FDA further allows the application of a variety of statistical analyses including PCA and ANOVA, as well as spatial interpolation methods. The approach we used is summarized in Figure 2 and described below. All steps were applied for spring and autumn data, independently.

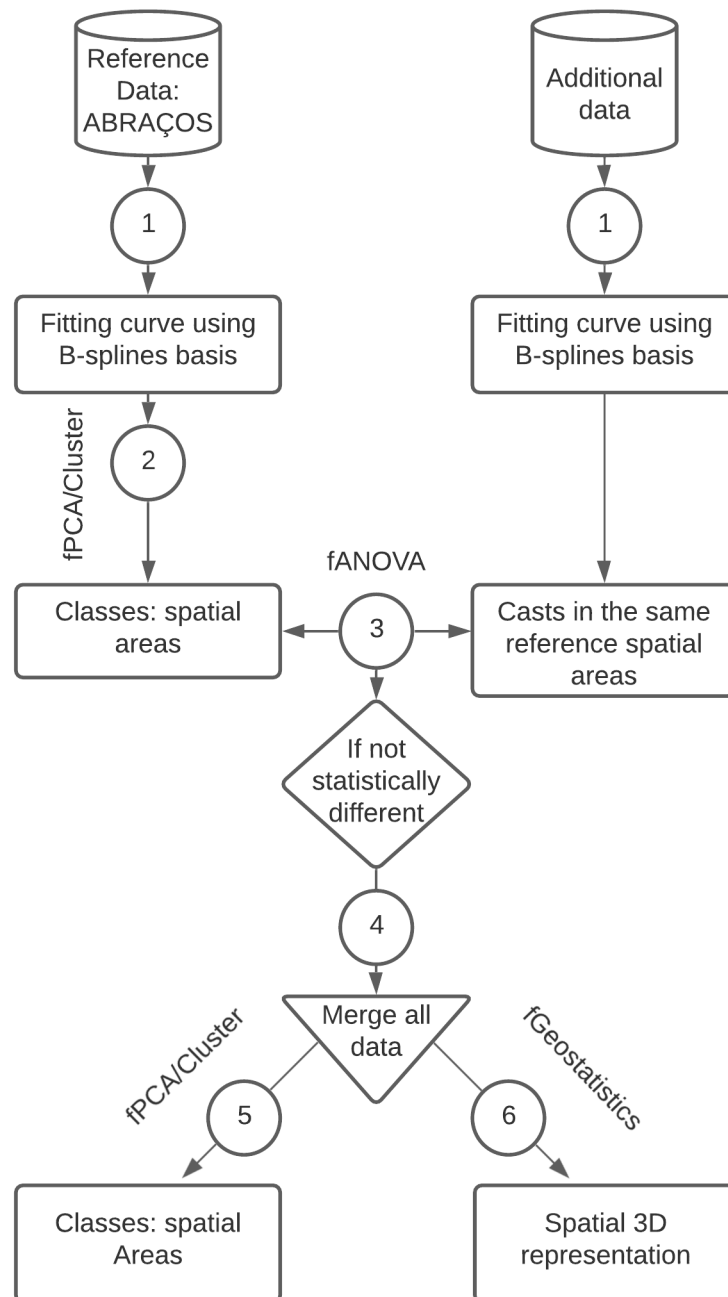


Figure 2 – Flowchart describing the Functional Data Analyses approach and the 3D representation of the oxygen content.

### 2.2.1. Fitting curves (B-spline)

The first step consists in transforming discrete DO profiles into functions (Fig. 2, step 1) (Ramsay and Silverman, 2005). For that we used a B-spline base function system of degree 3 (Boor, 2001), which is typically used for non-periodic curves and is defined by third degree polynomial segments joined end-to-end by placing a knot

at every observation point (Ramsay and Silverman, 2005; Ramsay et al., 2009). It is expressed as:

$$y_i = x_i(z) + \varepsilon_i \quad (1)$$

where  $(z_i, y_i)$ ,  $i=1, \dots, N$  are the data,  $z$  is depth and  $y$  is the DO,  $\varepsilon_i$  is the noise, expected to be as small as possible. The function  $x(z)$  is in the form of a linear combination of each basis function  $\phi_k(z)$ ,  $k=1, \dots, K$  such that:

$$x(z) = \sum_{k=1}^K c_k \phi_k(z) \quad (2)$$

where  $c_k$  are coefficients estimated by penalized regression using point wise data  $(z_1, y_1), \dots, (z_N, y_N)$  (Ramsay and Silverman, 2005).

Adjusting the function requires the best fit for the number of basis  $K$  and the roughness parameter  $\lambda$ , that must take into consideration the optimal balance between smoothing and interpolating the data. The number  $K$ -functions controls the flexibility of the spline, the higher, the more complexity is preserved. The roughness parameter  $\lambda$  allows continuous control over smoothness, to reduce the impact of noise when interpolating the data (Ramsay et al., 2009; Ramsay and Silverman, 2005). We first defined a range of possible potential  $K$  and  $\lambda$  based on the literature (Ramsay et al., 2009; Ramsay and Silverman, 2005). Then, a Generalised Cross Validation (GCV) was applied to estimate the actual optimal values within this range, using the R packages "fda" and "fda.usc" (Febrero-Bande and Fuente, 2012).

### **2.2.2. Characterising and comparing spatially ABRAÇOS and complementary datasets**

Once the DO profiles have been fitted as functions, the next step (Fig. 2, step 2) consisted in characterising the dominant modes of spatial variation of the ABRAÇOS dataset (reference data) by applying a functional Principal Component Analysis (fPCA; Ramsay and Silverman, 2005) and a hierarchical clustering (Cluster) achieved on the coefficients of the fPCA decomposition (Febrero-Bande and Fuente, 2012). The homogeneous groups of profiles were then plotted spatially to determine if they correspond to specific geographical areas.



Thereafter, in each homogeneous geographic areas defined from ABRAÇOS profiles, we applied a fANOVA (“fdanova” R package; Febrero-Bande and Fuente, 2012) to compare ABRAÇOS and complementary profiles (Fig. 2, step 3). Since no significant differences were observed between the reference and complementary profiles within each area from each season, we merged all the data to build a complete dataset with wider spatial coverage representative of spring and autumn canonical states (Fig. 2, step 4). Then fPCA, and Clustering was applied on the complete dataset (Fig. 2, step 5).

### **2.2.3. Functional Geostatistics – 3D representation**

To interpolate DO profiles in 3D (Fig. 2, step 6) we applied a functional Geostatistical Analysis (Giraldo et al., 2011). The use of functional ordinary kriging allows spatial predictions at non-data locations when the data values are functions. The predicted curve is a linear combination of data curves, with greater influence of the ones closer to the prediction point (Giraldo et al., 2011). For this method, we used the “fdagstat” R package (Grujic and Menafooglio, 2017, <https://github.com/ogru/fdagstat>).

To evaluate the quality of the resulting functional geostatistical models, we performed cross-validation analyses, in which we compared observed and predicted curves (Giraldo et al., 2011). We considered the Mean Square (MSD) differences i.e., the mean of the squared error between predicted and observed profiles (along depth) to evaluate the quality of the prediction. For that, we randomly removed 2% of the sampled curves (fitted with 30 basis K) and performed the functional Kriging predictor for the remaining 98% curves to predict the removed curves. This procedure was applied 51 and 61 times for ABRAÇOS 1 and ABRAÇOS 2 datasets, respectively, which is enough to cover all in situ sampled profiles.

## **3. Results**

fPCA and Cluster analyses revealed two significantly different areas for both ABRAÇOS 1 and 2 data (Fig. 3). One area corresponded to the northeast Brazil slope (Fig. 3, in blue) and the other to the Fernando de Noronha (FN) and Rocas Atoll (RA) area (Fig. 3, in green).

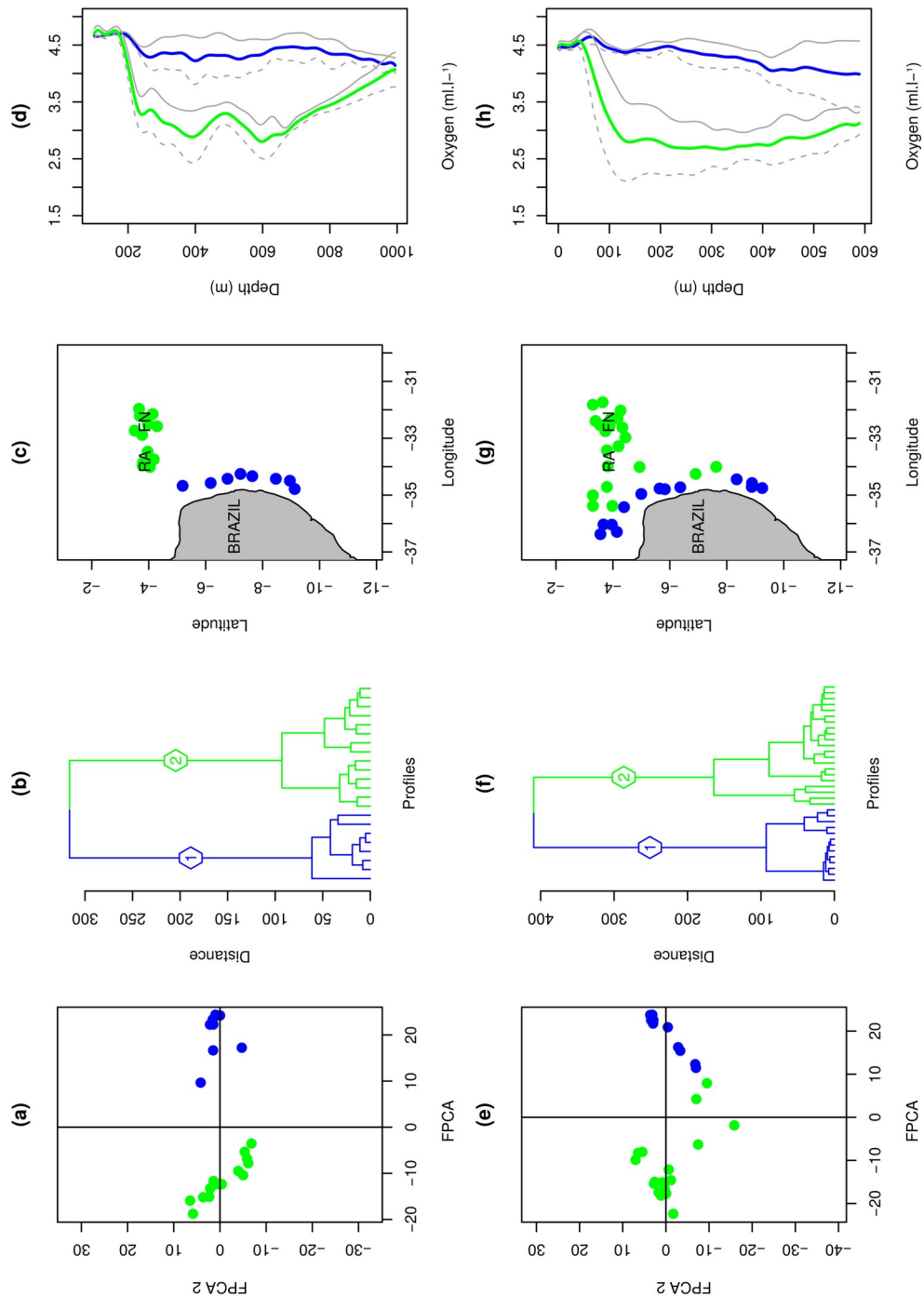


Figure 3 – Score of the first two fPCA components (a, e) and clustering (b, f) analyses achieved on DO profiles. Spatial distribution of the clusters (c, g) and mean DO profile for each area (d, h) with the variation over the mean profiles represented by the dashed and continuous lines. Spring: a-d; Autumn: e-h.

Since no significant differences (fANOVA,  $p > 0.05$ ; Supplementary Figure S1) were observed between ABRAÇOS and ancillary profiles within each classified area, we merged the datasets for each season, and we applied the fPCA and clustering

analyses on the complete datasets. Results depicted three distinct groups of DO profiles at both seasons (Fig. 4), representing three distinct spatial areas.

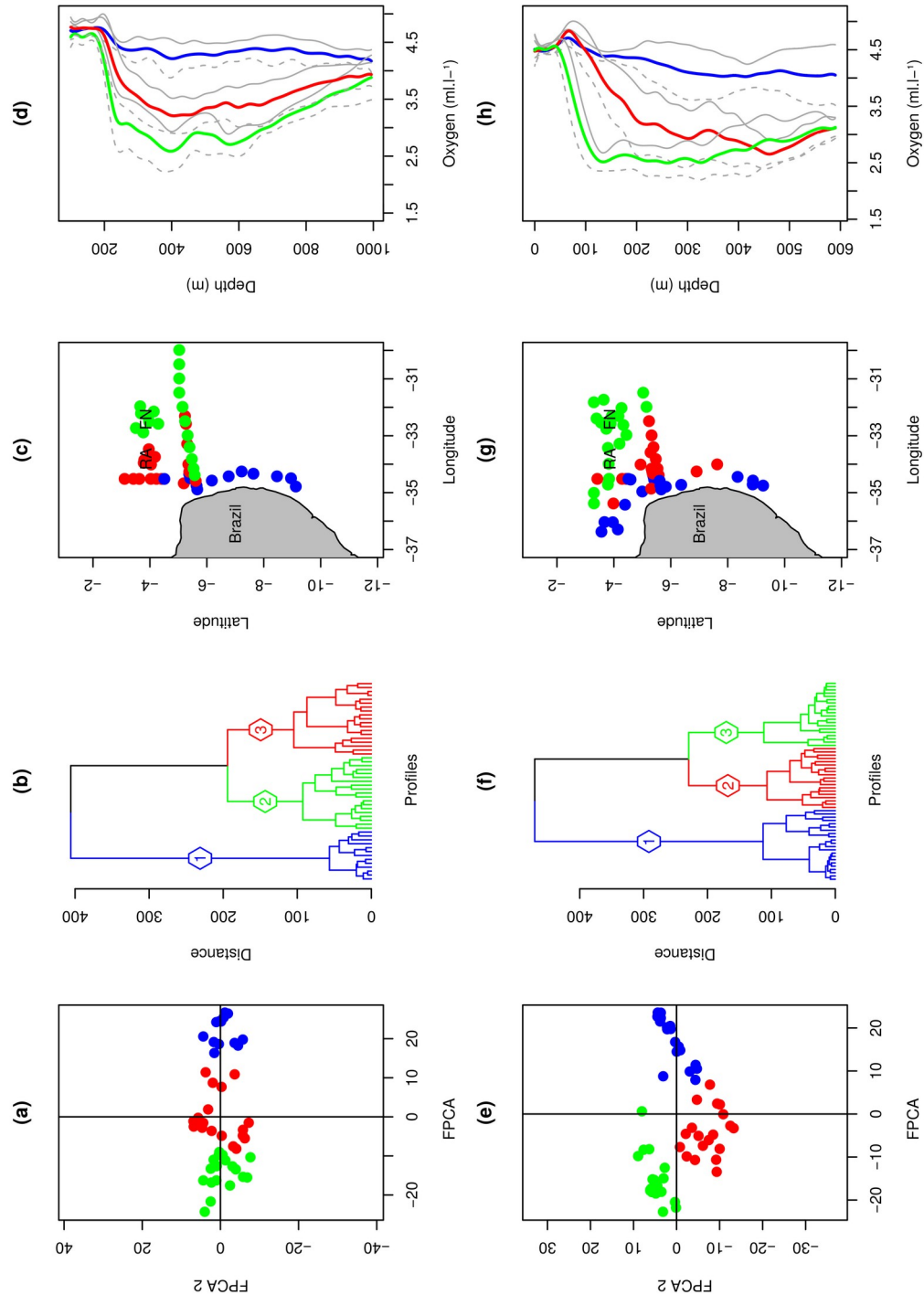


Figure 4 – Score of the first two fPCA components (a, e) and clustering (b, f) analyses achieved on DO profiles. Spatial distribution of the clusters (c, g) and mean DO profile for each area (d, h) with the variation over the mean profiles represented by the dashed and continuous lines. Spring: a-d; Autumn: e-h.

Group 1 was characterized by well oxygenated waters throughout the sampled water column. It was located along the slope under the influence of the WBCS. The mean DO content varied between 4.1 ml.l<sup>-1</sup> and 4.7 ml.l<sup>-1</sup> in spring (Fig. 4, d) and between 4 ml.l<sup>-1</sup> and 4.7 ml.l<sup>-1</sup> in autumn (Fig. 4, h).

The two other groups were characterised by a lower oxygen content. Group 3 presented the lower DO content among the three groups. Here referred to as the South Equatorial Current System (SECS) area, in our case, comprised by the surface cSEC (0-100 m) and the sub-surface SEUC (100-400 m). A steep oxycline was located at ~250 m depth in spring (DO: ~2.7 ml.l<sup>-1</sup>) and at ~125 m in autumn (DO: ~2.4 ml.l<sup>-1</sup>). Between the lower limit of oxycline and 600 m depth, DO content difference was ~0.4 ml.l<sup>-1</sup> in spring. A gradual increase in DO concentration from 3 ml.l<sup>-1</sup> to 3.8 ml.l<sup>-1</sup> was recorded down to 900 m deep. In autumn, the difference was ~0.27 ml.l<sup>-1</sup> between 125 and 425 m depth. DO increased below to reach 3.1 ml.l<sup>-1</sup> at 600 m deep.

Group 2 presented intermediary patterns of DO and was located between the two other groups (Fig 4. d, h), and therefore called the transition zone area. In spring, mean DO profiles were rather homogeneous between the surface and 175 m (4.7 ml.l<sup>-1</sup> – 3.6 ml.l<sup>-1</sup>), below a steeper gradient occurred between 175-250 m (3.6 ml.l<sup>-1</sup> – 3.3 ml.l<sup>-1</sup>), followed by a slow decrease in DO concentration to reach ~ 3.1 ml.l<sup>-1</sup> at 400 m. Then DO content increased smoothly, reaching 3.9 ml.l<sup>-1</sup> at 900 m depth. In autumn, profiles were marked by a slight increase between the surface and ~70 m (4.4 ml.l<sup>-1</sup> to 4.7 ml.l<sup>-1</sup>), followed by a decrease between 70 and ~450 m deep (from ~4.7 ml.l<sup>-1</sup> to ~2.6 ml.l<sup>-1</sup>). Below, DO increased up to 3.1 ml.l<sup>-1</sup> at ~600 m.

The extension of the well oxygenated waters associated to the WBCS varied seasonally (Fig. 4, c, d). For instance, at ~5.5°S, the limit between full oxygenated waters and the presence of deoxygenated waters in sub-surface (DO < 2.5 ml.l<sup>-1</sup>) was ~ 91 km from the coast in spring but was as close as 55 km in autumn.

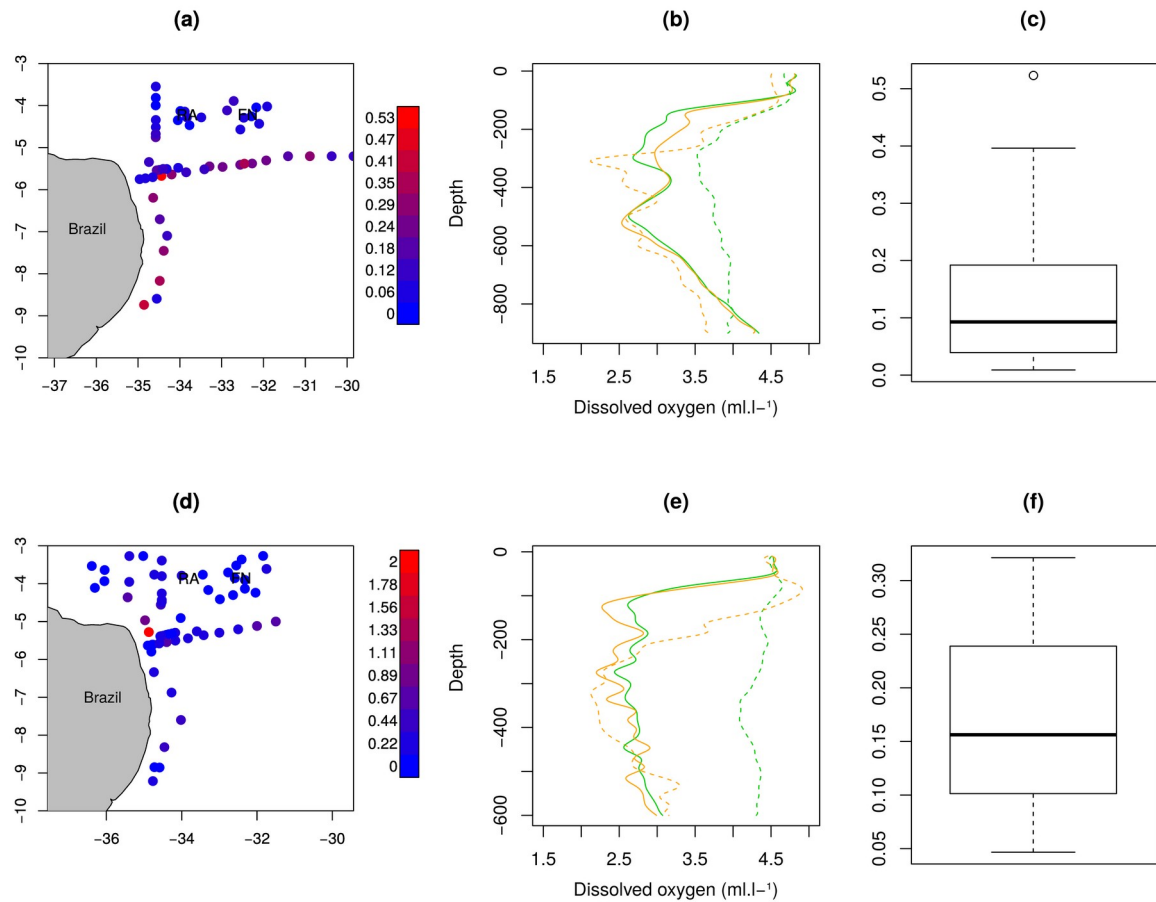


Figure 5 – Validation of Functional Ordinary Kriging of the DO profiles for spring (a, b, c) and autumn (d, e, f) using Mean Square Difference (MSD). Distribution of MSD for all DO profiles (a, d). Examples of good (emphasised blue dots, a, d; continuous green line, b, e) and poor (emphasised red dots, a, d; dashed green lines, b, e) predictions of observed DO profiles (orange lines) for spring (a, b) and autumn (d, e). Boxplots of the MSD between observed and predicted over/under all model predictions for both seasons (c, f).

The application of the functional geostatistical approach to reconstruct DO in 3D seems to provide robust results. Indeed, the MSD between observed and predicted smoothed curves showed an acceptable prediction by the variogram model (see Supplementary S2 for the fitting of the variogram) in all areas (Fig. 5). Results are described on the form of 2D at three selected depths (Fig. 6) and 3D interpolation over selected transects (Fig. 7).

**SPRING**

**AUTUMN**

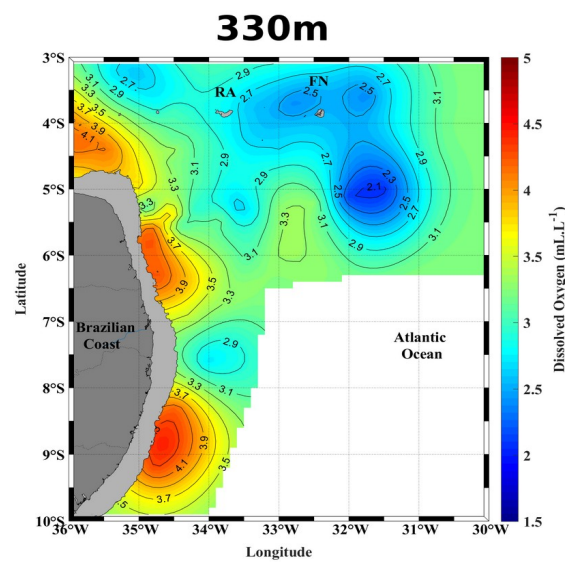
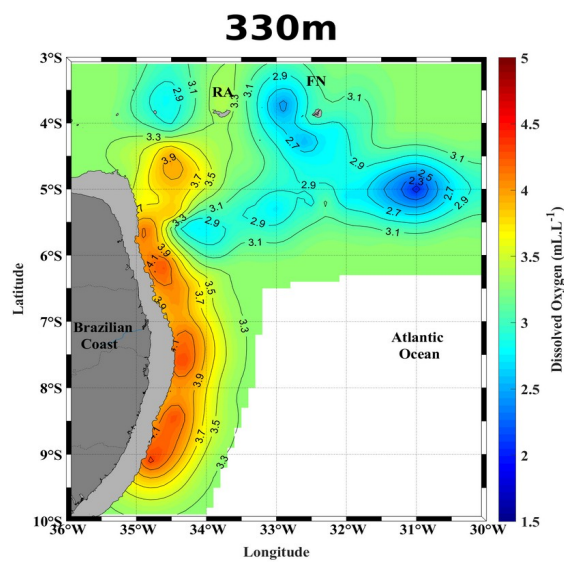
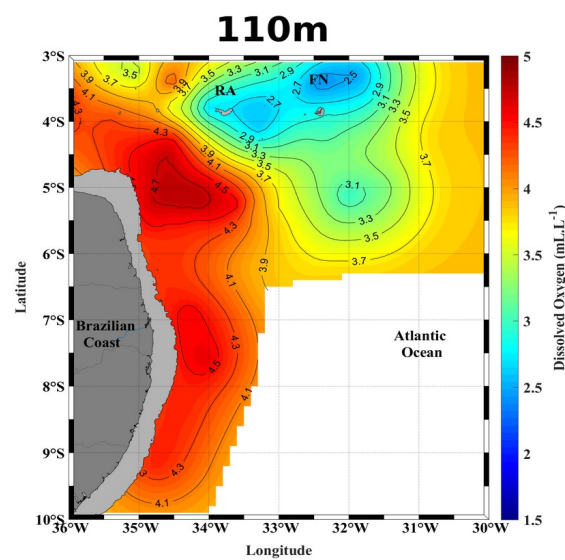
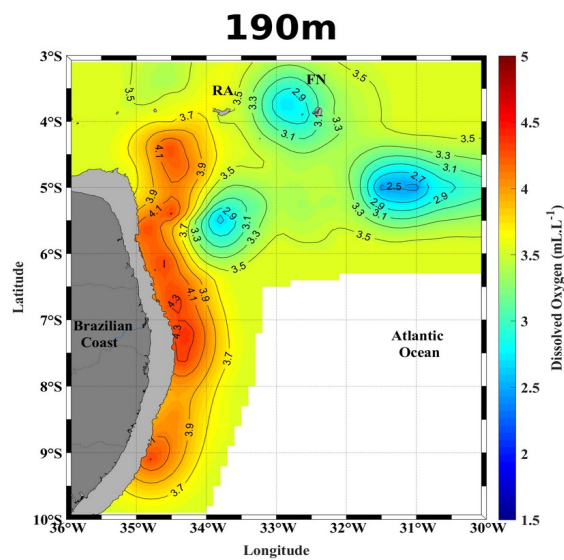
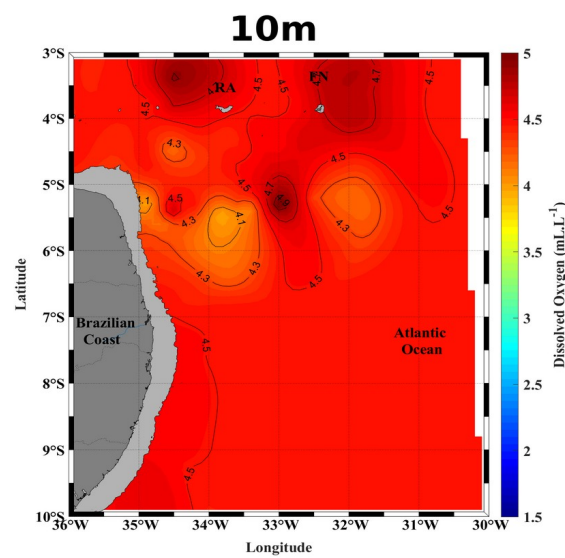
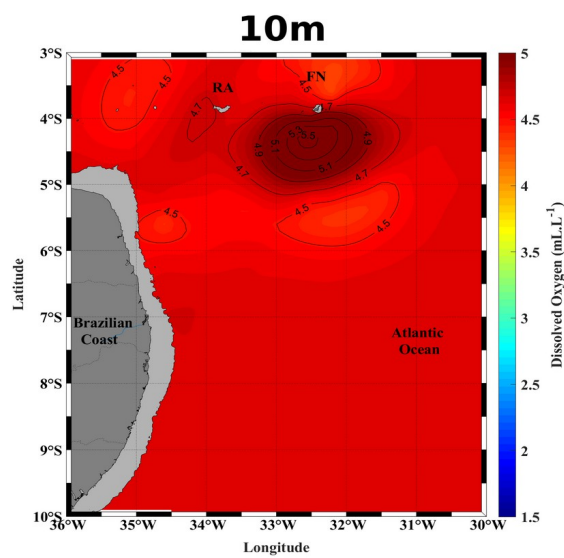


Figure 6 – Dissolved oxygen in spring (a, c, e) and autumn (b, d, f) at 10 m (a, b), 190 m (c), 110 m (d) and 330 m (e, f) in the SWTA. The continental shelf is limited by the 60 m isobath represented in light grey. RA: Rocas Atoll; FN: Fernando de Noronha archipelago. The oxygen scale varies from 1.5 ml.l<sup>-1</sup> to 5 ml.l<sup>-1</sup>.

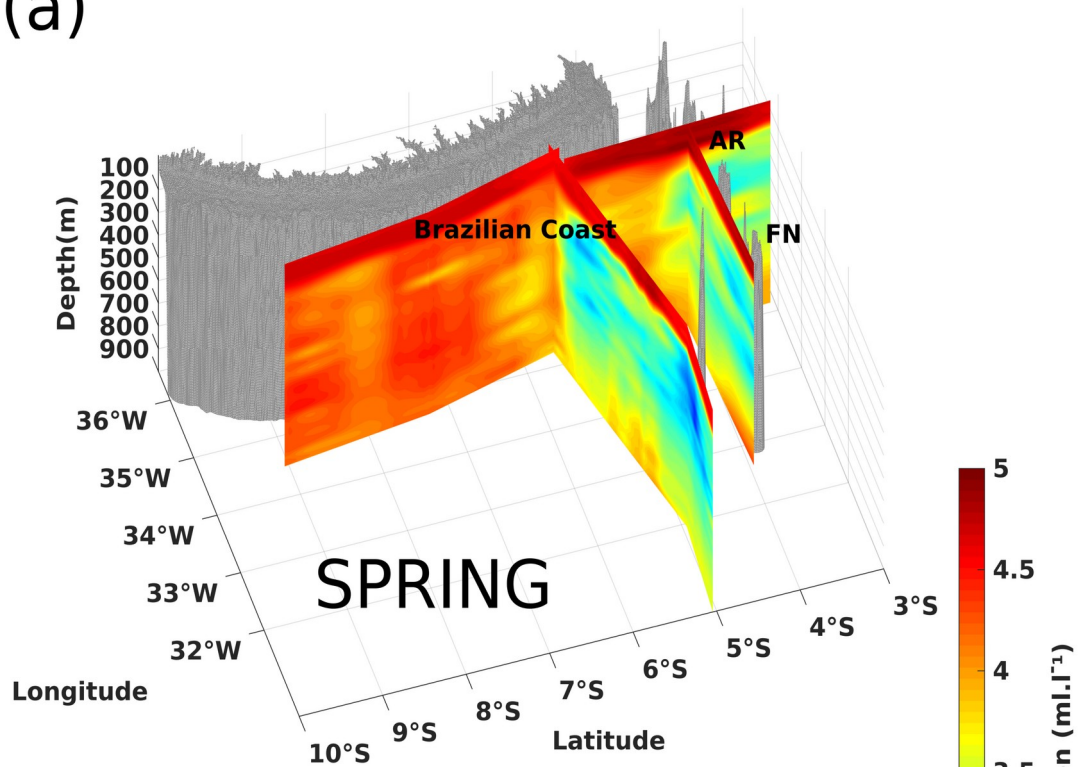
In the surface layer (~10 m; Fig. 6, a, b), the DO was homogeneous whatever the season (median: ~4.6 ml.l<sup>-1</sup> and ~4.4 ml.l<sup>-1</sup> in spring and autumn, respectively), except for slightly more oxygenated waters close to the coast north of ~5°S. Along the WBCS, the oxygenation remained high throughout the water column. We identified a front with a high oxygen gradient north of ~6°S at both seasons, with well oxygenated waters constrained against coast along the WBCS area, while the westernmost position of deoxygenated waters varied seasonally with the other two areas (Fig. 6; Fig. 7).

North of 5°S, a greater coverage of the SECS area was observed towards the west in autumn, while in spring it was delimited further east (around FN island) (Fig. 7). The upper limit of deoxygenated waters around FN was observed at shallower depths during autumn (110 m – north of FN; Fig. 6, d; Fig. 7, b) than spring (270 m – northwest of FN, Fig. 7, a). The transition zone area was wider in spring, covering the surroundings of RA, while narrower in autumn (Fig. 4, c). The low oxygen upper limit was at 190 m at the eastern end of the transition zone in spring (Fig. 6, c), while there was no observation of these waters in the area during autumn. South of 5°S the boundaries between the SECS and transition zone areas were better delimited in autumn than in spring (Fig. 4, c).

A larger coverage of deoxygenated waters over the transition zone and islands was observed at 330 m in both seasons (Fig. 6, e, f). There were no records of low DO below 400 m (450 m) during spring (autumn) (Fig. 7).



(a)



(b)

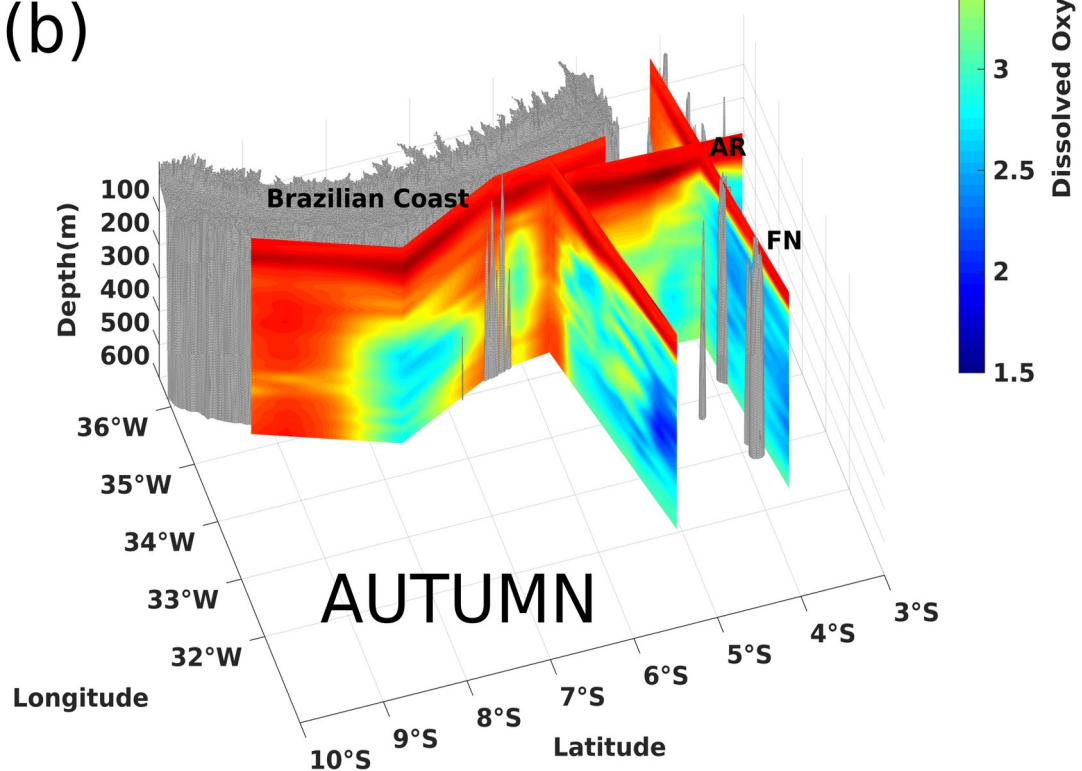


Figure 7 – 3D interpolation of DO using ordinary functional kriging. In spring (upper) interpolation relied on transects along-shelf ( $3.05^{\circ}\text{S}/34.75^{\circ}\text{W} - 7.25^{\circ}\text{S}/34.25^{\circ}\text{W}$  and  $7.25^{\circ}\text{S}/34.25^{\circ}\text{W} - 9.05^{\circ}\text{S}/34.30^{\circ}\text{W}$ ), along-shore ( $3.05^{\circ}\text{S}/34.65^{\circ}\text{W} - 5.55^{\circ}\text{S}/34.55^{\circ}\text{W}$ ), and cross-shore over the islands ( $4.05^{\circ}\text{S}/34.60^{\circ}\text{W} - 3.95^{\circ}\text{S}/32.15^{\circ}\text{W}$ ) and over the transition zone ( $4.95^{\circ}\text{S}/31.45^{\circ}\text{W} - 5.05^{\circ}\text{S}/29.95^{\circ}\text{W}$ ). In autumn (lower)



interpolation relied on transects along-shelf ( $4.95^{\circ}\text{S}/34.95^{\circ}\text{W} - 7.65^{\circ}\text{S}/34.30^{\circ}\text{W}$  and  $7.65^{\circ}\text{S}/34^{\circ}\text{W} - 9.25^{\circ}\text{S}/34.75^{\circ}\text{W}$ ), along-shore ( $3.45^{\circ}\text{S}/34.45^{\circ}\text{W} - 5.55^{\circ}\text{S}/34.55^{\circ}\text{W}$ ), and cross-shore over the islands ( $4.15^{\circ}\text{S}/36.25^{\circ}\text{W} - 3.65^{\circ}\text{S}/31.75^{\circ}\text{W}$ ) and over the transition zone ( $5.65^{\circ}\text{S}/34.85^{\circ}\text{W} - 5.05^{\circ}\text{S}/31.55^{\circ}\text{W}$ ). The grey areas represent the topography; RA: Rocas Atoll; FN: Fernando de Noronha archipelago.

#### 4. Discussion

Here, we provide a description of the DO content in the SWTA varying during spring and autumn seasons, directly linked to the current systems: (i) Western Boundary Current System (WBCS) area, characterized by well oxygenated waters; (ii) South Equatorial Current System (SECS) area, containing the lowest DO values among all, and (iii) transition zone area, with intermediate DO content. Previous studies showed that deoxygenated waters may enter the SWTA (Brandt et al., 2008, 2010, 2015; Hahn et al., 2017; Stramma et al., 2009) but they were too coarse to depict specific features. We reveal that while the water column is fully oxygenated in the NBUC/NBC, WBCS oxygen content decreases sharply at the limit of the NBUC/NBC core as close as  $\sim 91$  km ( $\sim 50$  km) from the coast in spring (autumn). Even with the westward transport of deoxygenated waters with the zonal current system (Brandt et al., 2008; Stramma and Schott, 1999), these low-oxygen structure seems to be limited outside of the boundaries of the northward NBUC/NBC flow.

We observed a greater advection of deoxygenated waters towards the west through the SECS area (Fig 4. g; Fig 7. b) in autumn. This agrees with the shallower and weaker NBUC core (Dossa et al., 2021) leading to a greater influence of the zonal equatorial current system towards the SWTA.

The extent of the well oxygenated surface layer varied spatially under the influence of the main circulation patterns observed in the SWTA. Around the RA and FN area, oxygen rich waters reach the lower limit of cSEC (Fig 6. c, d) (see also by Costa da Silva et al., 2021). Further west, the slightly higher oxygen content observed at  $\sim 5^{\circ}\text{S}$  close to the coast during both seasons (Fig. 7) may be influenced by the intensified oxygen rich NBUC/NBC flow. In fact, as the NBUC approaches its northwest inflection point ( $\sim 5.5^{\circ}\text{S}$  in spring and  $\sim 5.7^{\circ}\text{S}$  in autumn for our area) it no longer suffers the characteristic effects of high latitude dynamics that keep it at the subsurface, which leads to the NBUC/NBC system becoming shallower and more intense (Dossa et al., 2021). In addition, north of  $\sim 4.8^{\circ}\text{S}$ , at least in autumn, higher

DO content may be also related to the increased NBC flux, fed by the cSEC waters (Schott et al., 2003; Stramma et al., 1995).

The small seasonal variability of subsurface DO content observed in the WBCS area followed fluctuations in the intensity and vertical position of the NBUC core flow. Slightly lower DO values are associated with decreases in the intensity of the subsurface NBUC flow in spring, while higher oxygen concentrations happens during autumn, when NBUC core fluxes are stronger and deeper (Dossa et al., 2021).

In contrast to the WBCS area, the two other examined areas present a lower DO content in subsurface, below the cSEC. According to Costa da Silva et al. (2021), in the SECS area, the circulation below the cSEC is dominated by the eastward SEUC flows, which was observed to also encounter westward flows. We identified the presence of subsurface deoxygenated waters at the northwest (north) of FN during spring (autumn) only when SEUC flows were observed adjacent to the unknown westward flows. In the parts of the SEUC flow that did not encompass such westward flows, deoxygenated waters were not observed.

From previous works discussing the origin of the SEUC (Fischer, 2008; Hüttl-Kabus and Böning, 2008), we hypothesize that the importance of these westward flows on the presence of deoxygenated waters may be linked to internal recirculation between east-west equatorial current bands. If this is the case, a layer of complexity is added to the ongoing discussion about SEUC origin and how it affects the oxygen distribution in the SWTA. Indeed, the origin and variability of the western SEUC flow is still controversial. Some authors suggest that the SEUC is fed by water recirculation at its northernmost boundary, with only a small portion coming from the NBUC retroflexion (Schott et al., 1998; Brandt et al., 2006, Hüttl-Kabus and Bonning, 2008), while other works indicate a more continuous link between the high oxygen NBUC flow and the SEUC (Molinari, 1982; Arhan et al., 1998; Goes et al., 2005). These different assumptions indicate that the seasonality of the SEUC flow and that the NBUC retroflexion itself may be acting on the variation of DO content in SWTA.

Moving eastward, in the vicinity of RA, the south/southeastward NBUC flows were related to a retroflexion of the NBUC (Costa da Silva et al., 2021), in agreement with what was also found by Goes et al. (2005). According to our results,

this is in line with more oxygenated waters reaching RA during spring, in opposition to lower values found in autumn for the same depth. Furthermore, from the north-south variability of the SEUC core position in the SWTA (Costa da Silva et al., 2021; Dossa et al., 2021; Fischer et al., 2008), we hypothesize that a seasonal latitudinal displacement of the cSEC and SEUC cores could influence the distribution of these low oxygen waters. Based on this variability, compared to spring, the core of the cSEC and SEUC may move toward the south in the autumn, enabling the presence of deoxygenated waters from the SECS area further west. Oppositely, in spring, the northern position of the current cores would imply the positioning of these waters further east, around FN, allowing the NBUC retroflexion to occur over RA.

Results presented in here suggest that the NBUC/NBC system, regardless of the season, acts as a barrier to the presence of low oxygen waters into the shelf break towards the coast. The encounter of the well oxygenated WBCS waters with low oxygen waters found in the SECS forms a subsurface oxygen front in the SWTA boundary region.. In that sense, the NBUC retroflexion may also act as an expansion of the oxygen rich barrier formed by the NBUC/NBC system against the advance of westward deoxygenated waters over the continental shelf off northeast Brazil.

## 5. Conclusions

In this work, we use in situ measurements and FDA approach to obtain a comprehensive description of the DO distribution in the southwestern tropical Atlantic. Results proved satisfactory, especially with the condition of non-linearity of this type of data. The DO oceanscape constructed with this approach provide a precise vision of the distribution of low oxygen waters in the SWTA with the description of three distinct spatial regions, influenced seasonally by the variability of ocean circulation. In the WBCS area, the water column is fully oxygenated in the region of the core of the NBUC/NBC, decreasing at the limit of the core as close as ~91 km (~50 km) from the coast in spring (autumn). This pattern is related to the seasonal variability in NBUC/NBC flow. In opposition, the SECS area presents lower DO values, influenced by the westward transport of warmer and low DO waters by the equatorial currents (e.g., cSEC and eSEC).

Results also indicated that other processes are acting on the oxygen content in the study area, suggesting the influence of the variability of the NBUC connection to the SEUC flow. While NBUC retroflection during spring feed subsurface westward transport of DO rich waters, a seasonal latitudinal displacement of the SEUC core could influence the distribution of observed low oxygen waters. From the southward shift of the core in autumn, the low oxygen waters from the SECS area were observed further west, while the northward shift in spring would imply the positioning of these waters further east, around FN. Furthermore, the southward shift of the core would allow the NBUC retroflection to occur over RA region, corroborating with the records of low oxygen waters further east that we associated with more intense and deeper NBUC core in autumn.

Results presented and discussed in this work show that the NBUC/NBC system act as a barrier to the presence of westward deoxygenated waters entering the shelf break, and that the influence of this barrier on the region can vary seasonally. In this sense, we elucidate the importance of the NBUC/NBC system in oxygenating the WBCS area on a larger scale. Additionally, the occurrence of the NBUC retroflection, at least in spring, acted as an expansion of this barrier, positioning the deoxygenated waters further east.

## **Acknowledgments**

We acknowledge the French oceanographic fleet for funding the at-sea survey and the officers and crew of the R/V Antea for their contribution to the success of the operations during the ABRACOS cruises. J.G. thanks the support of the Coordenação de Aperfeiçoamento de Pessoal de Nível Superior (CAPES) through a Masters scholarship grant (88887.631474/2021-00). M.A. thanks the Brazilian Research Network on Global Climate Change - Rede CLIMA (FINEP-CNPq 437167/2016-0) and the Brazilian National Institute of Science and Technology for Tropical Marine Environments - INCT AmbTropic (CNPq/FAPESB 565054/2010-4 and 8936/2011) for their support. This work is a contribution to the International Joint Laboratory TAPIOCA ([www.tapioca.ird.fr](http://www.tapioca.ird.fr)) and to the TRIATLAS project, which has received funding from the European Union's Horizon 2020 research and innovation program under grant agreement No 817578.

## Disclosure Statement

No potential conflict of interest was reported by the authors.

## Funding

This work was supported by the Coordenação de Aperfeiçoamento de Pessoal de Nível Superior (CAPES) under Grant 88887.631474/2021-00.

## References

- Arhan, M., Mercier, H., Boulès, B., Gouriou, Y., 1998. Hydrographic sections across the Atlantic at 7°30N and 4°30S. *Deep Sea Research Part I: Oceanographic Research Papers* 45, 829–872. [https://doi.org/10.1016/S0967-0637\(98\)00001-6](https://doi.org/10.1016/S0967-0637(98)00001-6)
- Assunção, R.V., Silva, A.C., Roy, A., Boulès, B., Silva, C.H.S., TERNON, J.-F., Araujo, M., Bertrand, A., 2020. 3D characterisation of the thermohaline structure in the southwestern tropical Atlantic derived from functional data analysis of in situ profiles. *Progress in Oceanography* 187, 102399. <https://doi.org/10.1016/j.pocean.2020.102399>
- Bertrand, A., Chaigneau, A., Peraltilla, S., Ledesma, J., Graco, M., Monetti, F., Chavez, F.P., 2011. Oxygen: A Fundamental Property Regulating Pelagic Ecosystem Structure in the Coastal Southeastern Tropical Pacific. *PLoS ONE* 6, e29558. <https://doi.org/10.1371/journal.pone.0029558>.
- Bertrand, A., 2015. ABRACOS cruise. RV Antea. <http://dx.doi.org/10.17600/15005600>.
- Bertrand, A., 2017. ABRACOS 2 cruise. RV Antea. <http://dx.doi.org/10.17600/17004100>.
- Boor, C. De, 2001. A practical guide to splines. *Springer Handbooks Comput. Stat.* 302.
- Boulès, B., Gouriou, Y., Chuchla, R., 1999. On the circulation in the upper layer of the western equatorial Atlantic. *J. Geophys. Res.* 104, 21151–21170. <https://doi.org/10.1029/1999JC900058>
- Brandt, P., Bange, H.W., Banyte, D., Dengler, M., Didwischus, S.-H., Fischer, T., Greatbatch, R.J., Hahn, J., Kanzow, T., Karstensen, J., Körtzinger, A., Krahmann, G.,

Schmidtko, S., Stramma, L., Tanhua, T., Visbeck, M., 2015. On the role of circulation and mixing in the ventilation of oxygen minimum zones with a focus on the eastern tropical North Atlantic. *Biogeosciences* 12, 489–512. <https://doi.org/10.5194/bg-12-489-2015>

Brandt, P., Hormann, V., Boulès, B., Fischer, J., Schott, F.A., Stramma, L., Dengler, M., 2008. Oxygen tongues and zonal currents in the equatorial Atlantic. *J. Geophys. Res.* 113, C04012. <https://doi.org/10.1029/2007JC004435>

Brandt, P., Hormann, V., Körtzinger, A., Visbeck, M., Krahmann, G., Stramma, L., Lumpkin, R., Schmid, C., 2010. Changes in the Ventilation of the Oxygen Minimum Zone of the Tropical North Atlantic. *Journal of Physical Oceanography* 40, 1784–1801. <https://doi.org/10.1175/2010JPO4301.1>

Brandt, P., Schott, F.A., Provost, C., Kartavtseff, A., Hormann, V., Boulès, B., Fischer, J., 2006. Circulation in the central equatorial Atlantic: Mean and intraseasonal to seasonal variability. *Geophys. Res. Lett.* 33, L07609. <https://doi.org/10.1029/2005GL025498>

Breitburg, D., Levin, L.A., Oschlies, A., Grégoire, M., Chavez, F.P., Conley, D.J., Garçon, V., Gilbert, D., Gutiérrez, D., Isensee, K., Jacinto, G.S., Limburg, K.E., Montes, I., Naqvi, S.W.A., Pitcher, G.C., Rabalais, N.N., Roman, M.R., Rose, K.A., Seibel, B.A., Telszewski, M., Yasuhara, M., Zhang, J., 2018. Declining oxygen in the global ocean and coastal waters. *Science* 359, eaam7240. <https://doi.org/10.1126/science.aam7240>

Cochrane, J.D., Kelly, F.J., Olling, C.R., 1979. Subthermocline Countercurrents in the Western Equatorial Atlantic Ocean. *J. Phys. Oceanogr.* 9, 724–738. [https://doi.org/10.1175/1520-0485\(1979\)009<0724:SCITWE>2.0.CO;2](https://doi.org/10.1175/1520-0485(1979)009<0724:SCITWE>2.0.CO;2)

Costa da Silva, A., Chaigneau, A., Dossa, A.N., Eldin, G., Araujo, M., Bertrand, A., 2021. Surface Circulation and Vertical Structure of Upper Ocean Variability Around Fernando de Noronha Archipelago and Rocas Atoll During Spring 2015 and Fall 2017. *Front. Mar. Sci.* 8, 598101. <https://doi.org/10.3389/fmars.2021.598101>

da Silveira, I.C.A., Brown, W.S., Flierl, G.R., 2000. Dynamics of the North Brazil Current retroflexion region from the Western Tropical Atlantic Experiment

observations. J. Geophys. Res. 105, 28559–28583.  
<https://doi.org/10.1029/2000JC900129>

da Silveira, I.C.A., de Miranda, L.B., Brown, W.S., 1994. On the origins of the North Brazil Current. J. Geophys. Res. 99, 22501. <https://doi.org/10.1029/94JC01776>

Dossa, A.N., Silva, A.C., Chaigneau, A., Eldin, G., Araujo, M., Bertrand, A., 2021. Near-surface western boundary circulation off Northeast Brazil. Progress in Oceanography 190, 102475. <https://doi.org/10.1016/j.pocean.2020.102475>

Duteil, O., Oschlies, A., Böning, C.W., 2018. Pacific Decadal Oscillation and recent oxygen decline in the eastern tropical Pacific Ocean. Biogeosciences 15, 7111–7126. <https://doi.org/10.5194/bg-15-7111-2018>

Febrero-Bande, M., Fuente, M.O. de la, 2012. Statistical Computing in Functional Data Analysis: The R Package fda.usc. J. Stat. Soft. 51. <https://doi.org/10.18637/jss.v051.i04>

Fischer, J., Hormann, V., Brandt, P., Schott, F.A., Rabe, B., Funk, A., 2008. South Equatorial Undercurrent in the western to central tropical Atlantic. Geophys. Res. Lett. 35, L21601. <https://doi.org/10.1029/2008GL035753>

Gallo, N.D., Levin, L.A., 2016. Fish Ecology and Evolution in the World's Oxygen Minimum Zones and Implications of Ocean Deoxygenation, in: Advances in Marine Biology. Elsevier, pp. 117–198. <https://doi.org/10.1016/bs.amb.2016.04.001>

Giraldo, R., Delicado, P., Mateu, J., 2011. Ordinary kriging for function-valued spatial data. Environ Ecol Stat 18, 411–426. <https://doi.org/10.1007/s10651-010-0143-y>

Goes, M., Molinari, R., da Silveira, I., Wainer, I., 2005. Retroreflections of the North Brazil Current during February 2002. Deep Sea Research Part I: Oceanographic Research Papers 52, 647–667. <https://doi.org/10.1016/j.dsr.2004.10.010>

Grujic, O., Menafoglio, A., Yang, G., Caers, J., 2018. Cokriging for multivariate Hilbert space valued random fields: application to multi-fidelity computer code emulation. Stoch Environ Res Risk Assess 32, 1955–1971. <https://doi.org/10.1007/s00477-017-1486-9>

- Hahn, J., Brandt, P., Schmidtke, S., Krahmann, G., 2017. Decadal oxygen change in the eastern tropical North Atlantic. *Ocean Sci.* 13, 551–576. <https://doi.org/10.5194/os-13-551-2017>
- Hüttel-Kabus, S., Böning, C.W., 2008. Pathways and variability of the off-equatorial undercurrents in the Atlantic Ocean. *J. Geophys. Res.* 113, C10018. <https://doi.org/10.1029/2007JC004700>
- Karstensen, J., Stramma, L., Visbeck, M., 2008. Oxygen minimum zones in the eastern tropical Atlantic and Pacific oceans. *Progress in Oceanography* 77, 331–350. <https://doi.org/10.1016/j.pocean.2007.05.009>
- Keeling, R.F., Körtzinger, A., Gruber, N., 2010. Ocean Deoxygenation in a Warming World. *Annu. Rev. Mar. Sci.* 2, 199–229. <https://doi.org/10.1146/annurev.marine.010908.163855>
- Levin, L.A., 2018. Manifestation, Drivers, and Emergence of Open Ocean Deoxygenation. *Annu. Rev. Mar. Sci.* 10, 229–260. <https://doi.org/10.1146/annurev-marine-121916-063359>
- Löscher, C.R., Bange, H.W., Schmitz, R.A., Callbeck, C.M., Engel, A., Hauss, H., Kanzow, T., Kiko, R., Lavik, G., Loginova, A., Melzner, F., Meyer, J., Neulinger, S.C., Pahlow, M., Riebesell, U., Schunck, H., Thomsen, S., Wagner, H., 2016. Water column biogeochemistry of oxygen minimum zones in the eastern tropical North Atlantic and eastern tropical South Pacific oceans. *Biogeosciences* 13, 3585–3606. <https://doi.org/10.5194/bg-13-3585-2016>
- Luyten, J.R., Pedlosky, J., Stommel, H., 1983. The Ventilated Thermocline. *J. Phys. Oceanogr.* 13, 292–309. [https://doi.org/10.1175/1520-0485\(1983\)013<0292:TVT>2.0.CO;2](https://doi.org/10.1175/1520-0485(1983)013<0292:TVT>2.0.CO;2)
- Molinari, R.L., 1982. Observations of eastward currents in the tropical South Atlantic Ocean: 1978–1980. *J. Geophys. Res.* 87, 9707. <https://doi.org/10.1029/JC087iC12p09707>
- Molinari, R.L., Johns, E., 1994. Upper layer temperature structure of the western tropical Atlantic. *J. Geophys. Res.* 99, 18225. <https://doi.org/10.1029/94JC01204>



Oschlies, A., Brandt, P., Stramma, L., Schmidtko, S., 2018. Drivers and mechanisms of ocean deoxygenation. *Nature Geosci* 11, 467–473. <https://doi.org/10.1038/s41561-018-0152-2>

Prince, E.D., Luo, J., Phillip Goodyear, C., Hoolihan, J.P., Snodgrass, D., Orbesen, E.S., Serafy, J.E., Ortiz, M., Schirripa, M.J., 2010. Ocean scale hypoxia-based habitat compression of Atlantic istiophorid billfishes: Hypoxia-based habitat compression of billfishes. *Fisheries Oceanography* 19, 448–462. <https://doi.org/10.1111/j.1365-2419.2010.00556.x>

Ramsay, J., Hooker, G., Graves, S., 2009. Functional Data Analysis with R and MATLAB. Springer New York, New York, NY. <https://doi.org/10.1007/978-0-387-98185-7>

Ramsay, J.O., Silverman, B.W., 2005. Functional Data Analysis, Springer Series in Statistics. Springer New York, New York, NY. <https://doi.org/10.1002/0470013192.bsa239>

Ren, A.S., Chai, F., Xue, H., Anderson, D.M., Chavez, F.P., 2018. A Sixteen-year Decline in Dissolved Oxygen in the Central California Current. *Sci Rep* 8, 7290. <https://doi.org/10.1038/s41598-018-25341-8>

Ruiz-Medina, M.D., 2012. New challenges in spatial and spatiotemporal functional statistics for high-dimensional data. *Spatial Statistics* 1, 82–91. <https://doi.org/10.1016/j.spasta.2012.02.006>

Schmidtko, S., Stramma, L., Visbeck, M., 2017. Decline in global oceanic oxygen content during the past five decades. *Nature* 542, 335–339. <https://doi.org/10.1038/nature21399>

Schott et al. - 2003 - The zonal currents and transports at 35°W in the t.pdf, n.d.

Schott, F.A., Brandt, P., Hamann, M., Fischer, J., Stramma, L., 2002. On the boundary flow off Brazil at 5-10°S and its connection to the interior tropical Atlantic: ON THE BOUNDARY FLOW OFF BRAZIL. *Geophys. Res. Lett.* 29, 21-1-21–4. <https://doi.org/10.1029/2002GL014786>

Schott, F.A., Dengler, M., Brandt, P., Affler, K., Fischer, J., Boulès, B., Gouriou, Y., Molinari, R.L., Rhein, M., 2003. The zonal currents and transports at 35°W in the

tropical Atlantic: ZONAL CURRENTS AND TRANSPORTS AT 35 DEGREES W. *Geophys. Res. Lett.* 30. <https://doi.org/10.1029/2002GL016849>

Schott, F.A., Fischer, J., Stramma, L., 1998. Transports and Pathways of the Upper-Layer Circulation in the Western Tropical Atlantic. *J. Phys. Oceanogr.* 28, 1904–1928. [https://doi.org/10.1175/1520-0485\(1998\)028<1904:TAPOTU>2.0.CO;2](https://doi.org/10.1175/1520-0485(1998)028<1904:TAPOTU>2.0.CO;2).

Shepherd, J.G., Brewer, P.G., Oschlies, A., Watson, A.J., 2017. Ocean ventilation and deoxygenation in a warming world: introduction and overview. *Phil. Trans. R. Soc. A.* 375, 20170240. <https://doi.org/10.1098/rsta.2017.0240>

Stramma, L., Fischer, J., Reppin, J., 1995. The North Brazil Undercurrent. *Deep Sea Research Part I: Oceanographic Research Papers* 42, 773–795. [https://doi.org/10.1016/0967-0637\(95\)00014-W](https://doi.org/10.1016/0967-0637(95)00014-W)

Stramma, L., Johnson, G.C., Sprintall, J., Mohrholz, V., 2008. Expanding Oxygen-Minimum Zones in the Tropical Oceans. *Science* 320, 655–658. <https://doi.org/10.1126/science.1153847>

Stramma, L., Schott, F., 1999. The mean flow field of the tropical Atlantic Ocean. *Deep Sea Research Part II: Topical Studies in Oceanography* 46, 279–303. [https://doi.org/10.1016/S0967-0645\(98\)00109-X](https://doi.org/10.1016/S0967-0645(98)00109-X)

Stramma, L., Visbeck, M., Brandt, P., Tanhua, T., Wallace, D., 2009. Deoxygenation in the oxygen minimum zone of the eastern tropical North Atlantic. *Geophys. Res. Lett.* 36, L20607. <https://doi.org/10.1029/2009GL039593>

Tsuchiya, M., 1986. Thermostads and circulation in the upper layer of the Atlantic Ocean. *Progress in Oceanography* 16, 235–267. [https://doi.org/10.1016/0079-6611\(86\)90040-6](https://doi.org/10.1016/0079-6611(86)90040-6)

Vaquer-Sunyer, R., Duarte, C.M., 2008. Thresholds of hypoxia for marine biodiversity. *PNAS* 105, 15452–15457. <https://doi.org/10.1073/pnas.0803833105>

## Supplementary figures

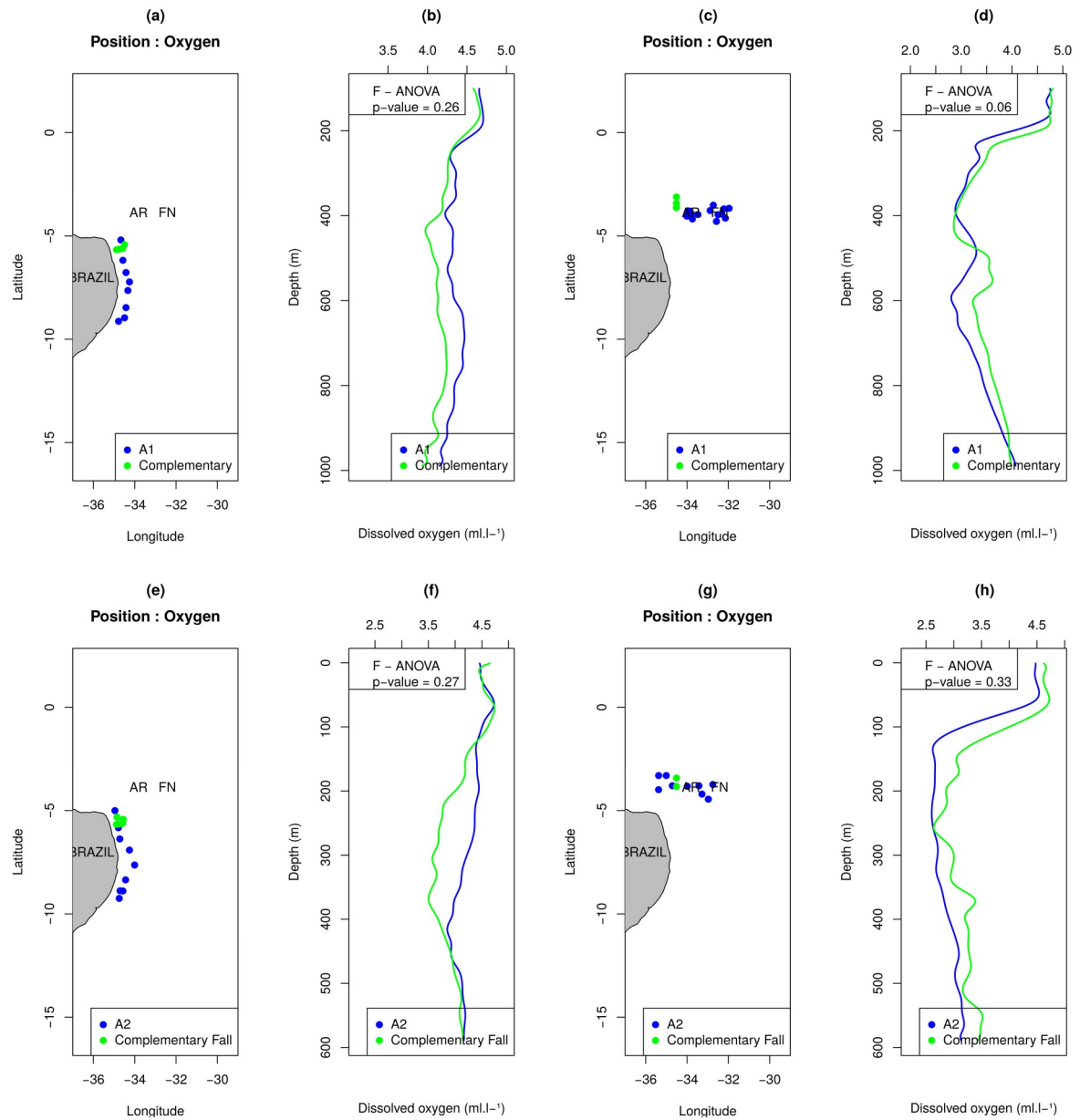


Figure S1 – Functional ANOVA (spring: b, d; autumn: f, h) between the DO profiles from different databases (spring: a, c; autumn: e, g) within each area classified from the reference dataset.

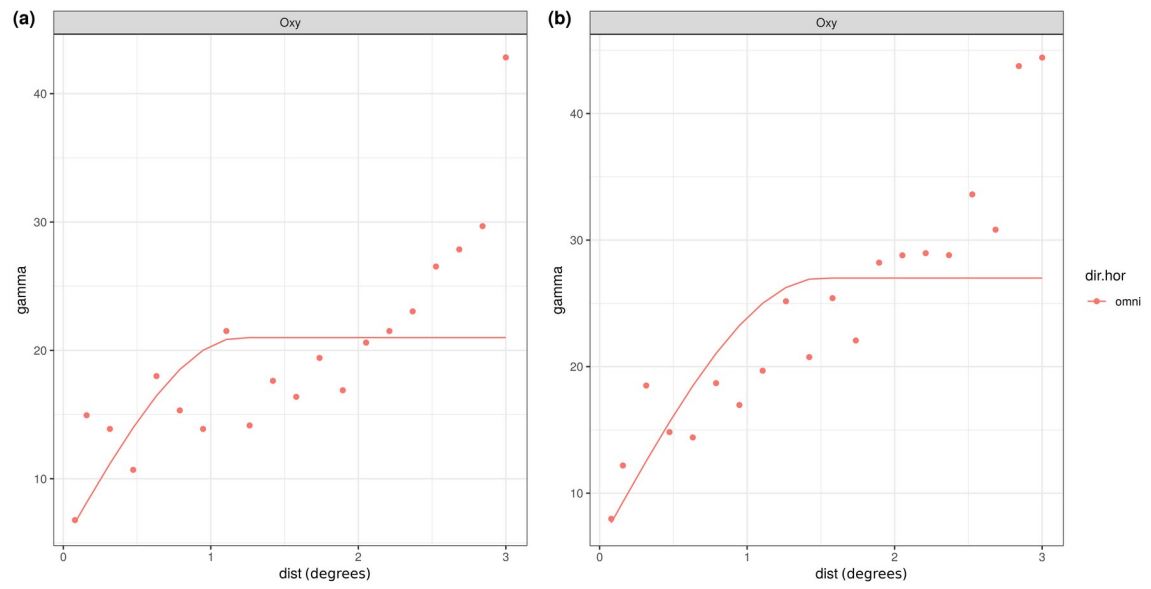


Figure S2 – Variogram for Functional Ordinary Kriging in spring (left) and autumn (right).

## 4 FINAL CONSIDERATIONS

The use of in situ measurements and FDA approach to obtain a comprehensive description of the DO distribution in the southwestern tropical Atlantic has led to satisfactory results, especially with the condition of non-linearity of this type of data. The DO oceanscape constructed provide an accurate view, with the description of three distinct spatial regions, seasonally influenced by the variability of ocean circulation.

Results also indicated that other processes are acting on the oxygen content, suggesting the influence of the variability of the NBUC connection to the SEUC flow. While NBUC retroflection during spring feed subsurface westward transport of DO rich waters, a seasonal latitudinal displacement of the SEUC core could influence the distribution of observed low oxygen waters. From the southward shift of the core in autumn, the low oxygen waters from the SECS area were observed further west, while the northward shift in spring would imply the positioning of these waters further east, around FN. Furthermore, the southward shift of the core would allow the NBUC retroflection to occur over RA region, corroborating with the records of low oxygen waters further east that we associated with more intense and deeper NBUC core in autumn.

Results presented and discussed in this work show that the NBUC/NBC system act as a barrier, that can vary seasonally, to the presence of westward deoxygenated waters entering the shelf break. In this sense, we elucidate the importance of the NBUC/NBC system in oxygenating the WBCS area on a larger scale. Additionally, the occurrence of the NBUC retroflection, at least in spring, acted as an expansion of this barrier, positioning the deoxygenated waters further east.

## REFERENCES

- ARHAN, M; MERCIER, H; BOURLÈS, B; *et al.* Hydrographic sections across the Atlantic at 7°30N and 4°30S. **Deep Sea Research Part I: Oceanographic Research Papers**, v. 45, n. 6, p. 829–872, 1998.
- ASSUNÇÃO, Ramilla V.; SILVA, Alex C.; ROY, Amédée; *et al.* 3D characterisation of the thermohaline structure in the southwestern tropical Atlantic derived from functional data analysis of in situ profiles. **Progress in Oceanography**, v. 187, p. 102399, 2020.
- BERTRAND, A.; BALLÓN, M.; CHAIGNEAU, A. Acoustic observation of living organisms reveals the upper limit of the oxygen minimum zone. **PLoS ONE**, v. 5, n. 4, 2010.
- BERTRAND, Arnaud; CHAIGNEAU, Alexis; PERALTILLA, Salvador; *et al.* Oxygen: A Fundamental Property Regulating Pelagic Ecosystem Structure in the Coastal Southeastern Tropical Pacific. **PLoS ONE**, v. 6, n. 12, p. e29558, 2011.
- BERTRAND, Arnaud. ABRACOS cruise. RV Antea, 2015
- BERTRAND, Arnaud. ABRACOS 2 cruise. RV Antea, 2017
- BOOR, Carl. **A practical guide to splines**. Springer Handbooks Comput. Stat. 302.
- BOURLÈS, B.; GOURIOU, Y.; CHUCHLA, R. On the circulation in the upper layer of the western equatorial Atlantic. **Journal of Geophysical Research: Oceans**, v. 104, n. C9, p. 21151–21170, 1999.
- BRANDT, P.; BANGE, H. W.; BANYTE, D.; *et al.* On the role of circulation and mixing in the ventilation of oxygen minimum zones with a focus on the eastern tropical North Atlantic. **Biogeosciences**, v. 12, n. 2, p. 489–512, 2015.
- BRANDT, Peter; HORMANN, Verena; BOURLÈS, Bernard; *et al.* Oxygen tongues and zonal currents in the equatorial Atlantic. **Journal of Geophysical Research**, v. 113, n. C4, p. C04012, 2008.
- BRANDT, Peter; HORMANN, Verena; KÖRTZINGER, Arne; *et al.* Changes in the Ventilation of the Oxygen Minimum Zone of the Tropical North Atlantic. **Journal of Physical Oceanography**, v. 40, n. 8, p. 1784–1801, 2010.
- BRANDT, Peter; SCHOTT, Friedrich A.; PROVOST, Christine; *et al.* Circulation in the central equatorial Atlantic: Mean and intraseasonal to seasonal variability. **Geophysical Research Letters**, v. 33, n. 7, p. L07609, 2006.
- BREITBURG, Denise; LEVIN, Lisa A.; OSCHLIES, Andreas; *et al.* Declining oxygen in the global ocean and coastal waters. **Science**, v. 359, n. 6371, p. eaam7240, 2018.

COCHRANE, John D.; KELLY, Francis J.; OLLING, Charles R. Subthermocline Countercurrents in the Western Equatorial Atlantic Ocean. **Journal of Physical Oceanography**, v. 9, n. 4, p. 724–738, 1979.

COSTA DA SILVA, Alex; CHAIGNEAU, Alexis; DOSSA, Alina N.; *et al.* Surface Circulation and Vertical Structure of Upper Ocean Variability Around Fernando de Noronha Archipelago and Rocas Atoll During Spring 2015 and Fall 2017. **Frontiers in Marine Science**, v. 8, p. 598101, 2021.

DA SILVEIRA, Ilson C. A.; BROWN, Wendell S.; FLIERL, Glenn R. Dynamics of the North Brazil Current retroflection region from the Western Tropical Atlantic Experiment observations. **Journal of Geophysical Research: Oceans**, v. 105, n. C12, p. 28559–28583, 2000.

DA SILVEIRA, Ilson C. A.; DE MIRANDA, Luiz B.; BROWN, Wendell S. On the origins of the North Brazil Current. **Journal of Geophysical Research**, v. 99, n. C11, p. 22501, 1994.

DOSSA, Alina N.; SILVA, Alex C.; CHAIGNEAU, Alexis; *et al.* Near-surface western boundary circulation off Northeast Brazil. **Progress in Oceanography**, v. 190, p. 102475, 2021.

DUTEIL, Olaf; OSCHLIES, Andreas; BÖNING, Claus W. Pacific Decadal Oscillation and recent oxygen decline in the eastern tropical Pacific Ocean. **Biogeosciences**, v. 15, n. 23, p. 7111–7126, 2018.

FEBRERO-BANDE, Manuel; FUENTE, Manuel Oviedo de la. Statistical Computing in Functional Data Analysis: The R Package **fda.usc**. **Journal of Statistical Software**, v. 51, n. 4, 2012. Disponível em: <<http://www.jstatsoft.org/v51/i04/>>. Acesso em: 23 fev. 2022.

FISCHER, Jürgen; HORMANN, Verena; BRANDT, Peter; *et al.* South Equatorial Undercurrent in the western to central tropical Atlantic. **Geophysical Research Letters**, v. 35, n. 21, p. L21601, 2008.

GALLO, N.D.; LEVIN, L.A. Fish Ecology and Evolution in the World's Oxygen Minimum Zones and Implications of Ocean Deoxygenation. *In*: **Advances in Marine Biology**. [s.l.]: Elsevier, 2016, v. 74, p. 117–198. Disponível em: <<https://linkinghub.elsevier.com/retrieve/pii/S0065288116300013>>. Acesso em: 23 fev. 2022.

GIRALDO, R.; DELICADO, P.; MATEU, J. Ordinary kriging for function-valued spatial data. **Environmental and Ecological Statistics**, v. 18, n. 3, p. 411–426, 2011.

GOES, Marlos; MOLINARI, Robert; DA SILVEIRA, Ilson; *et al.* Retroflections of the North Brazil Current during February 2002. **Deep Sea Research Part I: Oceanographic Research Papers**, v. 52, n. 4, p. 647–667, 2005.

GRUJIC, Ognjen; MENAFOGLIO, Alessandra; YANG, Guang; *et al.* Cokriging for multivariate Hilbert space valued random fields: application to multi-fidelity computer

code emulation. **Stochastic Environmental Research and Risk Assessment**, v. 32, n. 7, p. 1955–1971, 2018.

HAHN, Johannes; BRANDT, Peter; SCHMIDTKO, Sunke; *et al.* Decadal oxygen change in the eastern tropical North Atlantic. **Ocean Science**, v. 13, n. 4, p. 551–576, 2017.

HÜTTL-KABUS, Sabine; BÖNING, Claus W. Pathways and variability of the off-equatorial undercurrents in the Atlantic Ocean. **Journal of Geophysical Research**, v. 113, n. C10, p. C10018, 2008.

KARSTENSEN, Johannes; STRAMMA, Lothar; VISBECK, Martin. Oxygen minimum zones in the eastern tropical Atlantic and Pacific oceans. **Progress in Oceanography**, v. 77, n. 4, p. 331–350, 2008.

KEELING, Ralph F.; KÖRTZINGER, Arne; GRUBER, Nicolas. Ocean Deoxygenation in a Warming World. **Annual Review of Marine Science**, v. 2, n. 1, p. 199–229, 2010.

LEVIN, Lisa A. Manifestation, Drivers, and Emergence of Open Ocean Deoxygenation. **Annual Review of Marine Science**, v. 10, n. 1, p. 229–260, 2018.

LÖSCHER, Carolin R.; BANGE, Hermann W.; SCHMITZ, Ruth A.; *et al.* Water column biogeochemistry of oxygen minimum zones in the eastern tropical North Atlantic and eastern tropical South Pacific oceans. **Biogeosciences**, v. 13, n. 12, p. 3585–3606, 2016.

LUYTEN, J. R.; PEDLOSKY, J.; STOMMEL, H. The Ventilated Thermocline. **Journal of Physical Oceanography**, v. 13, n. 2, p. 292–309, 1983.

MOLINARI, Robert L. Observations of eastward currents in the tropical South Atlantic Ocean: 1978–1980. **Journal of Geophysical Research**, v. 87, n. C12, p. 9707, 1982.

MOLINARI, Robert L.; JOHNS, Elizabeth. Upper layer temperature structure of the western tropical Atlantic. **Journal of Geophysical Research**, v. 99, n. C9, p. 18225, 1994.

NAQVI, S. W. A. *et al.* Seasonal oxygen deficiency over the western continental shelf of India. In: Past and present water column anoxia. Springer, Dordrecht, 2006. p.195–224.

OSCHLIES, Andreas; BRANDT, Peter; STRAMMA, Lothar; *et al.* Drivers and mechanisms of ocean deoxygenation. **Nature Geoscience**, v. 11, n. 7, p. 467–473, 2018.

PAULY, Daniel; KINNE, Otto. **Gasping fish and panting squids: oxygen, temperature and the growth of water-breathing animals**. Oldendorf/Luhe, Germany: International Ecology Institute, 2010.



PRAETORIUS, S. K. et al. North Pacific deglacial hypoxic events linked to abrupt ocean warming. *Nature*, v. 527, n. 7578, 2015.

PRINCE, Eric D.; LUO, Jiangang; PHILLIP GOODYEAR, C.; *et al.* Ocean scale hypoxia-based habitat compression of Atlantic istiophorid billfishes: Hypoxia-based habitat compression of billfishes. **Fisheries Oceanography**, v. 19, n. 6, p. 448–462, 2010.

RAMSAY, J. O.; SILVERMAN, B. W. **Functional Data Analysis**. New York, NY: Springer New York, 1997. (Springer Series in Statistics). Disponível em: <<http://link.springer.com/10.1007/978-1-4757-7107-7>>. Acesso em: 23 fev. 2022.

RAMSAY, James; HOOKER, Giles; GRAVES, Spencer. **Functional Data Analysis with R and MATLAB**. New York, NY: Springer New York, 2009. Disponível em: <<http://link.springer.com/10.1007/978-0-387-98185-7>>. Acesso em: 23 fev. 2022.

REN, Alice S.; CHAI, Fei; XUE, Huijie; *et al.* A Sixteen-year Decline in Dissolved Oxygen in the Central California Current. **Scientific Reports**, v. 8, n. 1, p. 7290, 2018.

RHEIN, M. et al. Ventilation variability of Labrador Sea Water and its impact on oxygen and anthropogenic carbon: a review. *Philosophical Transactions of the Royal Society A: Mathematical, Physical and Engineering Sciences*, v. 375, n. 2102, p. 20160321, 2017.

RUIZ-MEDINA, M.D. New challenges in spatial and spatiotemporal functional statistics for high-dimensional data. **Spatial Statistics**, v. 1, p. 82–91, 2012.

SCHMIDTKO, Sunke; STRAMMA, Lothar; VISBECK, Martin. Decline in global oceanic oxygen content during the past five decades. **Nature**, v. 542, n. 7641, p. 335–339, 2017.

SCHOTT, Friedrich A.; BRANDT, Peter; HAMANN, Meike; *et al.* On the boundary flow off Brazil at 5-10°S and its connection to the interior tropical Atlantic: ON THE BOUNDARY FLOW OFF BRAZIL. **Geophysical Research Letters**, v. 29, n. 17, p. 21-1-21-4, 2002.

SCHOTT, Friedrich A.; DENGLER, Marcus; BRANDT, Peter; *et al.* The zonal currents and transports at 35°W in the tropical Atlantic: ZONAL CURRENTS AND TRANSPORTS AT 35 DEGRESS W. **Geophysical Research Letters**, v. 30, n. 7, 2003. Disponível em: <<http://doi.wiley.com/10.1029/2002GL016849>>. Acesso em: 7 mar. 2022.

SCHOTT, Friedrich A.; FISCHER, Jürgen; STRAMMA, Lothar. Transports and Pathways of the Upper-Layer Circulation in the Western Tropical Atlantic. **Journal of Physical Oceanography**, v. 28, n. 10, p. 1904–1928, 1998.

SEIBEL, Brad A. Critical oxygen levels and metabolic suppression in oceanic oxygen minimum zones. **Journal of Experimental Biology**, v. 214, n. 2, p. 326-336, 2011.

SHEPHERD, John G.; BREWER, Peter G.; OSCHLIES, Andreas; *et al.* Ocean ventilation and deoxygenation in a warming world: introduction and overview. **Philosophical Transactions of the Royal Society A: Mathematical, Physical and Engineering Sciences**, v. 375, n. 2102, p. 20170240, 2017.

STRAMMA, Lothar; FISCHER, Jürgen; REPPIN, Jörg. The North Brazil Undercurrent. **Deep Sea Research Part I: Oceanographic Research Papers**, v. 42, n. 5, p. 773–795, 1995.

STRAMMA, Lothar; JOHNSON, Gregory C.; SPRINTALL, Janet; *et al.* Expanding Oxygen-Minimum Zones in the Tropical Oceans. **Science**, v. 320, n. 5876, p. 655–658, 2008.

STRAMMA, Lothar; SCHOTT, Friedrich. The mean flow field of the tropical Atlantic Ocean. **Deep Sea Research Part II: Topical Studies in Oceanography**, v. 46, n. 1–2, p. 279–303, 1999.

STRAMMA, Lothar; VISBECK, Martin; BRANDT, Peter; *et al.* Deoxygenation in the oxygen minimum zone of the eastern tropical North Atlantic. **Geophysical Research Letters**, v. 36, n. 20, p. L20607, 2009.

TSUCHIYA, Mizuki. Thermostads and circulation in the upper layer of the Atlantic Ocean. **Progress in Oceanography**, v. 16, n. 4, p. 235–267, 1986.

VAQUER-SUNYER, Raquel; DUARTE, Carlos M. Thresholds of hypoxia for marine biodiversity. **Proceedings of the National Academy of Sciences**, v. 105, n. 40, p. 15452–15457, 2008.